Tampere University

Joona Lappalainen

COSMIC RAY FAILURES IN POWER SEMICONDUCTORS

Master of Science Thesis
Faculty of Information Technology and Communication Sciences
Supervisors: Assoc. Prof. Tomi Roinila, D.Sc. Tatu Musikka
Examiners: Assoc. Prof. Tomi Roinila, Doctoral Researcher Joni Markkula
December 2022

ABSTRACT

Joona Lappalainen: Cosmic Ray Failures in Power Semiconductors
Master of Science Thesis
Tampere University
Master's Programme in Electrical Engineering
December 2022

Cosmic rays are particles radiating from the galaxy to the earth. From these particles, high-energy neutrons are seen to cause failures when they collide with the base nuclei in power semiconductors. These collisions can trigger different failure mechanisms depending on the component type. Moreover, the failures are random and occur within nanoseconds without any prior sign.

This thesis introduces cosmic ray failures as a phenomenon in power semiconductors, the affecting factors, the estimation of failure probabilities, and existing testing procedures. Also, a test setup with natural terrestrial radiation was developed to compare test results from artificial radiation sources. Lastly, methods to improve the cosmic ray robustness of power semiconductors were discussed.

The affecting factors are the blocking voltage, junction temperature, altitude, and radiation flux. The voltage was seen to be the most effective factor because when a certain voltage threshold is achieved, the failure rates increase exponentially. The junction temperature and altitude can be included in the estimation of failure probability with formulas composed of experimental data. Lastly, radiation flux was seen to be dependent on solar activity, latitude, and altitude.

For quantifying cosmic ray failures, three different empirical models were presented. Comparison between these models showed differences and indicated the need for testing with real hardware to get accurate failure rates. However, these models as well as Monte Carlo techniques and TCAD simulations were noted to help in the early phase of development to adjust the radiation robustness.

The test setup developed in this thesis was the first step for cosmic ray testing at Danfoss Drives. The setup included multiple IGBT power modules with the gates short-circuited to ensure a blocking state. During the test, a high collector-emitter voltage was applied constantly. Six failures occurred during the test and showed a good match to the estimation from accelerated tests.

Regarding the methods for reducing cosmic ray failures, adjusting the width of the drift region was seen to be effective. Also, surrounding the components with neutron-attenuating materials seemed to decrease the probability of failures. Lastly, some previous research results were combined in the comparison of silicon and silicon carbide. It seemed that the latter should be more robust supporting the trend of using silicon carbide in high-voltage applications.

Keywords: cosmic ray, power semiconductor, failure mechanism, IGBT, power MOSFET, diode

TIIVISTELMÄ

Joona Lappalainen: Kosmisen säteilyn aiheuttama vikaantuminen tehopuolijohteissa
Diplomityö
Tampereen yliopisto
Sähkötekniikan DI-ohjelma
Joulukuu 2022

Kosminen säteily tarkoittaa avaruudesta maahan säteileviä hiukkasia. Näistä hiukkasista korkeaenergisten neutronien nähdään aiheuttavan vikoja tehopuolijohteissa, kun ne törmäävät tehopuolijohteiden atomiytimiin. Nämä törmäykset voivat laukaista erilaisia vikamekanismeja komponenttityypistä riippuen. Lisäksi viat ovat satunnaisia ja tapahtuvat nanosekunneissa ilman mitään varoitusta.

Tässä diplomityössä esitetään kosmisen säteilyn aiheuttama vikaantuminen yhtenä vikamekanismina tehopuolijohteissa. Vikaantumismekanismiin liittyen selvitetään siihen vaikuttavat tekijät, keinot ennustaa vikaantumisen todennäköisyys sekä mahdolliset testausmenetelmät. Lisäksi kehitetään testausjärjestelmä, jossa komponentit altistetaan jännitteisinä luonnolliselle säteilylle. Testituloksia vertaillaan komponenttivalmistajan hiukkaskiihdyttimillä tehtyjen testien tuloksiin. Lopuksi selvitetään menetelmiä, joilla voi parantaa tehopuolijohteiden säteilykestoisuutta.

Vikaantumisen todennäköisyyteen vaikuttavia tekijöitä ovat estotilan jännite, liitoslämpötila, korkeus meren pinnasta ja säteilyvuo, jolle puolijohde altistuu. Jännite nähtiin vaikuttavimpana tekijänä, sillä kun tietty jännitekynnys saavutetaan, vikaantumistahti kasvaa eksponentiaalisesti. Liitoslämpötila ja korkeus voidaan huomioida vikaantumistahdin estimoinnissa käyttämällä empiiriseen dataan perustuvia kaavoja. Viimeisenä, säteilyvuon nähtiin riippuvan auringon aktiivisuudesta, maan päällisistä koordinaateista sekä korkeudesta meren pinnasta.

Vikaantumistahdin määrittämiseen esitellään kolme empiiriseen dataan perustuvaa laskentamallia. Tulosten vertailussa näiden mallien välillä nähtiin suuria eroja, joka johtaa tarpeeseen saada komponentteja testattavaksi, jotta saadaan realistisia tuloksia. Nämä mallit ovat kuitenkin hyödyllisiä puolijohdekomponenttien suunnittelun alkuvaiheessa ja näitä tukemaan on kehitetty Monte Carlo -tekniikkaa ja TCAD-simulaatiomalleja, jotka ottavat paremmin huomioon puolijohteiden rakenteen.

Tässä työssä kehitetty testijärjestelmä oli ensimmäinen askel kosmisen säteilyn aiheuttamaan vikaantumistestaukseen Danfoss Drivesissa. Testikokoonpano sisälsi useita IGBT-tehomoduuleja, joiden hilat oli oikosuljettu estotilan varmistamiseksi. Testissä moduulit altistettiin jatkuvalle korkealle kollektori-emitterijännitteelle. Testin aikana ilmeni kuusi vikaantumista, joista laskettu vikaantumistahti vastasi hyvin moduulivalmistajan arviota kiihdytettyjen testien perusteella.

Säteilykestoisuuden parantamiseen liittyen, drift-alueen paksuudella nähtiin merkittävä vaikutus vikaantumistodennäköisyyteen. Lisäksi tehopuolijohteiden suojaamisen neutronisäteilyä vaimentavilla materiaaleilla nähtiin vähentävän vikaantumisia. Lopuksi vertailtiin puolijohteissa käytettävien materiaalien, piin ja piikarbidin säteilykestoisuutta. Nähtiin, että piikarbidin pitäisi olla kestävämpi, mikä tukee niiden käyttöönottoa tulevaisuuden korkean jännitteen applikaatioissa.

Avainsanat: kosminen säteily, tehopuolijohde, vikaantumismekanismi, IGBT, teho MOSFET, diodi

PREFACE

This thesis was written for Danfoss Drives, whose products use power semiconductors. It was interesting to study a subject that sounded so absurd to me in the beginning. Seeing results from the developed test setup was exciting, and I am happy about the good discussions this subject raised with the people I was working with.

First, I would like to thank Tatu Musikka and Ari Ristimäki for their shared knowledge and excellent guidance during my work. Thanks to my co-workers for creating a great working environment and proposing interesting research ideas for this thesis. Also, thanks to Tomi Roinila from the University of Tampere for the great feedback and practical help. Finally, thanks to my friends and family for supporting me throughout my studies. It has been a rewarding experience.

Vaasa, 5 December 2022

Joona Lappalainen

CONTENTS

LIST OF SYMBOLS AND ABBREVIATIONS

ANITA	atmospheric-like neutrons from thick target
CAL	controlled axial lifetime
CIA	current-induced avalanche
DN	Deep-N buffer layer
DUT	device under test
FEM	finite element method
FIT	failure in time
FWD	freewheeling diode
IC	integrated circuit
IGBT	insulated-gate bipolar transistor
LANSCE	Los Alamos Neutron Science Center
LET	linear energy transfer
MCNP	Monte Carlo N-Particle
MOSFET	metal-oxide-semiconductor field-effect transistor
MTTF	mean time to failure
NPC	neutral point clamped
NPT	non-punch through
NYC	New York City
PID	proportional–integral–derivative
PSI	Paul Scherrer Institute
PT	punch through
PWM	pulse-width modulation
QARM	Qinetic Atmospheric Radiation Model
RCNP	Research Center for Nuclear physics
SEB	single-event burnout
TCAD	Technology Computer-Aided Design

E_{av}	spatially averaged electric field
P_f	total device failure rate
P_{lf}	local device section failure rate
R_B	body region spreading resistance
T_0	temperature constant
t_i	time of fail
T_j	junction temperature
T_{SUM}	number of device-fluence product
V_{aval}	avalanche voltage
V_{CE}	collector-emitter voltage
V_{DC}	direct current voltage
V_{DS}	drain-source voltage
Δf_i	fluence-to-fail
A	area
E	electric field
h	altitude
i	sum over failure events
r	number of failures of devices
Si	silicon
SiC	silicon-carbide
ε	permittivity
λ	failure in time
ρ	net charge density
Ω	device volume

1. INTRODUCTION

Cosmic rays are particles radiated from the galaxy to the earth. These rays are called primary rays until they reach the earth, where they collide with the atmosphere's air molecules and produce secondary rays such as electrons, protons, neutrons, pions, photons, and muons [1]. From these particles, high-energy neutrons have been seen to cause failures when they collide with base nuclei in power semiconductors.

Cosmic ray failures have been under research in power semiconductors since the first failure findings in the early 1990s. These failures occurred randomly during the blocking state of devices and could not be explained by the knowledge at that time. Further research to find an explanation for this phenomenon proceeded [2] in different environments. High DC voltage in the blocking direction was applied both in a lab above ground and in an underground salt mine. It was seen that no failures occurred in the mine whereas multiple failures were reported in the lab. These failures have later been justified as cosmic ray failures which are in power electronics denoted as single-event burnouts (SEB) [3].

Failures caused by cosmic rays are a major factor for device reliability and need to be considered throughout the development phase of a power semiconductor device. One of the main goals of power semiconductor development is to optimize performance while dealing with a tradeoff between electrical parameters and radiation robustness. This makes it incredibly important to understand the physics behind these failures and to be able to estimate radiation robustness for different designs as early as possible.

This thesis was done to get insight into cosmic ray failures as a phenomenon and how they could affect the power semiconductor modules used in power converters. Failure rates had previously been estimated in reference conditions when in real applications the chance for failure could change depending on operating parameters like voltage profile, temperature, altitude, latitude, and solar activity. Taking these factors into account, a test setup to test radiation robustness for power semiconductor modules was developed. The thesis was requested by Danfoss Drives operating in Vaasa.

The thesis begins with a brief introduction to the history of cosmic ray failures and a further look into the physics behind this failure mechanism. The failure mechanism is different depending on the type of power semiconductor and different designs have been

seen to improve the cosmic ray robustness of the device [4]. In this thesis, diodes, power metal-oxide-semiconductor field-effect transistors (MOSFETs), and insulated-gate bipolar transistors (IGBTs) are selected for research as they are the most common power electronic devices used in high-power converters.

The second topic of the thesis considers factors affecting cosmic ray failures, of which the blocking state voltage, junction temperature, and neutron flux are the most significant. Some models have been proposed to calculate temperature and altitude factors, but voltage dependency is more difficult to calculate as it highly depends on the device design. Cosmic ray failures increase with higher voltages and neutron fluxes but decrease at higher temperatures [3]. Thus, taking voltage profiles and the environment into account when estimating failure rates is a matter of importance.

The third topic of the thesis considers calculation and simulation methods for this failure method. These are essential development steps that should always be done before expensive testing for real devices. Three known calculation models by Kaminski [5], Pfirsch [6], and Zeller [7] are presented. Also, simulation models have been developed to understand the temperature and current behavior when cosmic rays are present [6]. However, a precise model for MOSFET and IGBT is still under research because of their complex structure [3].

The fourth topic in this thesis is the testing and failure rate estimation for cosmic ray-induced failures from the results. Testing this failure method can be tricky as it is difficult to see whether the failure is caused by cosmic rays or not. Also, the testing is time-consuming. Some accelerated tests have succeeded at laboratories located in high altitudes in the Alps [8, 9], but the time taken to do these tests was not feasible and could not be done for low failure in time (FIT) rates. Highly ionized proton beams with similar energies to neutron beams have been developed to accelerate the testing even further [10, 11, 12]. These test results can then be compared to natural neutron flux and get a correction factor to conclude a realistic failure rate estimate. A test setup in this thesis was developed to do cosmic ray failure testing with a natural neutron flux.

Lastly, methods to improve radiation robustness for power semiconductor devices, such as shielding and chip design adjustments, are presented. One aspect of this topic is to consider different base materials, such as silicon (Si) and silicon-carbide (SiC). This is relevant as when higher voltage applications are to take place, Si IGBTs are planned to be replaced by SiC MOSFETs. From this topic, along with the others, the most significant findings are concluded to finish the thesis regarding this somewhat declamatory but interesting phenomenon.

2. COSMIC RAY FAILURES

In the early 1990s, a new random failure mode was found for power semiconductors. This failure was causing a series of failures with random time intervals, making the single failure event unpredictable. The fast failure time and no prior signs of leakage current before the fault led researchers to suppose radioactive decay in either silicon or metallization (aluminum) or cosmic rays as the possible failure cause. Further investigation to find the failure cause was succeeded in [2] and cosmic rays were concluded as the cause for failure. These days cosmic ray failure, also known as SEB failure, is a well-known phenomenon among power semiconductor manufacturers when reliability is discussed.

Through system-level tradeoffs, it might be possible to reach the reliability goal at a lower cost. This requires an understanding of the cosmic ray risks and extra effort but should be succeeded whenever possible as it makes the design more optimized. Some of these tradeoffs and radiation robustness improving designs will be discussed below.

Cosmic radiation coming from space is considered primary radiation which consists of energetic nuclear fragments. These nuclear fragments collide with air molecules when they reach the atmosphere and form so-called secondary radiation, which consists of elementary particles such as electrons, muons, pions, and nucleons. Of the latter, 90% are neutrons, which are the most important particles regarding cosmic ray failures. These neutrons might get energies of several GeV (giga-electron volt) in space but at terrestrial altitudes, they split their energies in cascades. [12] A picture of primary radiation splitting into secondary radiation in the atmosphere is presented below.

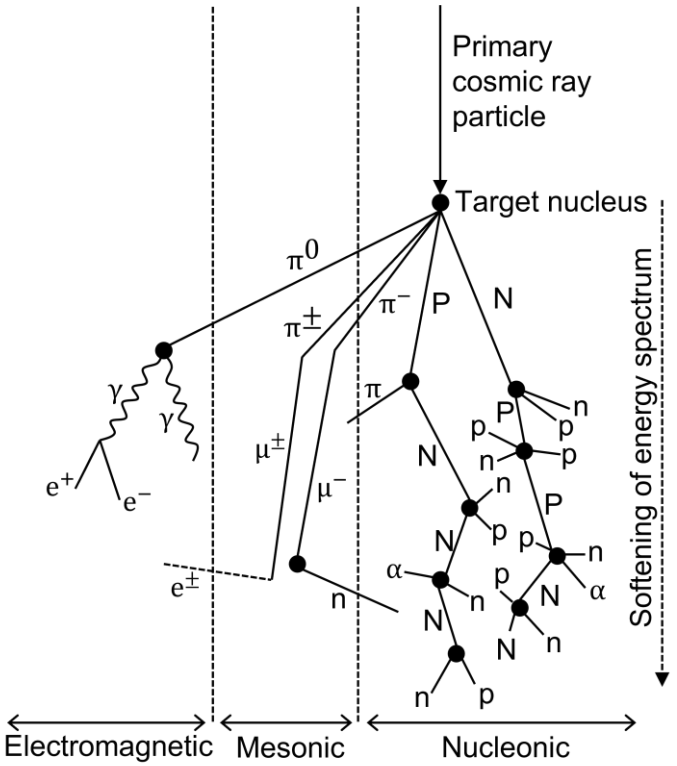

Figure 1. *The formation of secondary radiation in the atmosphere [13]*

In Figure 1, cascades of secondary particles are visible, and it is also notable that the spallation products mainly keep their direction. Regarding cosmic ray failures, nucleonic particles are of interest, and electromagnetic and mesonic radiation are ignored because of their low amount at terrestrial altitudes. Neutrons are marked as *n*, protons as *p* and protons carrying the nuclear cascade as *P*, alpha particles as *α*, electrons and positrons as $e^{\pm}$, gamma-ray photons as *γ*, pions as *π*, and muons as *μ*.

2.1 Origin

As the name defines, cosmic rays originate from cosmic space. Different sources of radiation consisting of high-energy particles are acknowledged. Depending on the energy of the particles, sources like the sun, supernova eruptions, and cores of distant active galaxies are considered the main origins. The sun is told to produce most of the radiation up to 10 GeV and the particles with even higher energy are from supernova eruptions and distant galaxies. [3]

Cosmic ray flux in space is about 100 000/m^2/sec and at sea level, the nucleon flux is about 360/m^2/sec [1]. This indicates that only a few of the particles in space have enough energy to penetrate the earth's atmosphere. At terrestrial altitudes, particle energies below 100 MeV are claimed to be responsible for most of the larger bursts of charge in silicon [14]. On the other hand, [12] claims that the charge bursts happen because of

neutron particles with energies between 50 MeV and 200 MeV. These varying visions indicate the difficulty to justify cosmic ray failures.

2.2 Mechanism

Failure mechanism has been under heavy research in recent years to give an understanding of what causes SEB failure in power semiconductors such as diodes, power MOSFETs, and IGBTs. Diodes, in general, are considered an easier approach to failure study. They do not have the parasitic bipolar transistor structure, that is included in power MOSFETs (Figure 5) and IGBTs (Figure 6), which would make the analysis more difficult [12]. However, studies on these controllable power electronic devices exist.

The cosmic ray failure mechanism gets its origin most likely from neutrons or protons, but pions and muons must be considered as well. Failures tend to happen in the high-field region when the power electronic chip is in a blocking state, also known as “off-state”. On earth, neutrons can have high energies and go through power semiconductors but only a small part of them collide with the base material nucleus, e.g. silicon or silicon carbide. This collision transfers energy to the nucleus and causes a locally dense plasma of charge carriers. The electrical field is forced out of the plasma and spikes of electric fields are formed at the boundary of the plasma region. When a certain electric field threshold is reached, more carriers are produced than are diffused out of the plasma region. Through this self-sustaining process to generate enough carriers (impact ionization), a streamer is produced, which short-circuits the blocking region of the device and leads to destruction [15]. These streamers have been reported to occur for a 3-10 ns duration [16]. However, not all streamers are destructive. In fact, non-destructive streamers have been stated to be rather common. This is demonstrated in Figure 2 edited from [17] for a diode, but the same principle applies to power MOSFET and IGBT. [3, 4, 12]

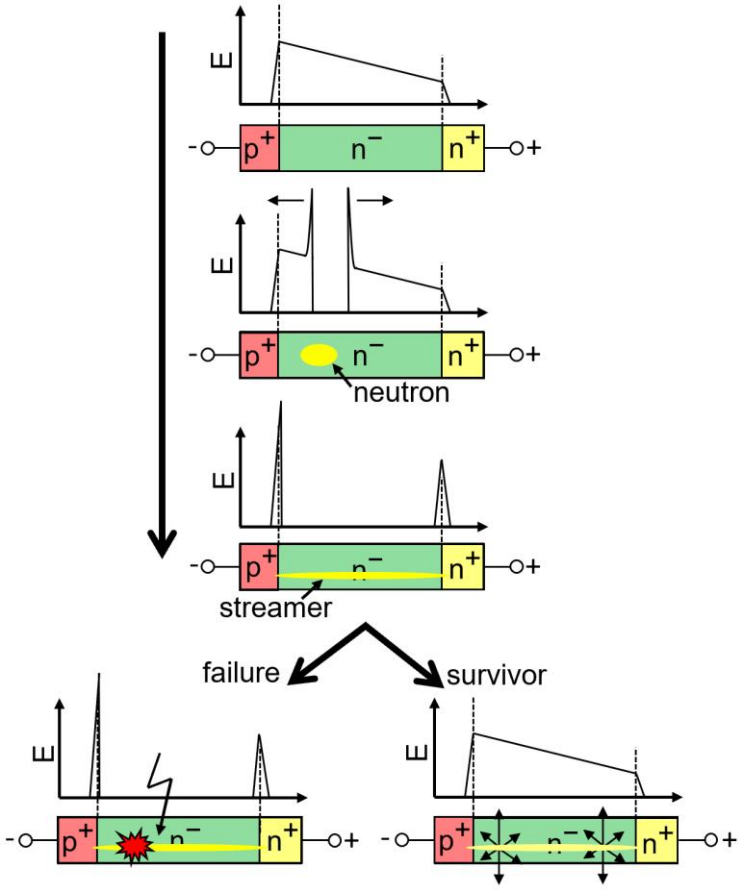

Figure 2. *Step-by-step destruction of a diode by a neutron, the same principle applies to IGBT and power MOSFET*

Cosmic ray failures from field data are difficult to track as when a semiconductor device gets destroyed, analysis to find the cause for the failure can be difficult. However, laboratory tests for cosmic ray failures have succeeded and small pinholes have been found in failed devices [3]. For example, from destroyed diodes, a pinhole and a molten area were observed (Figure 3).

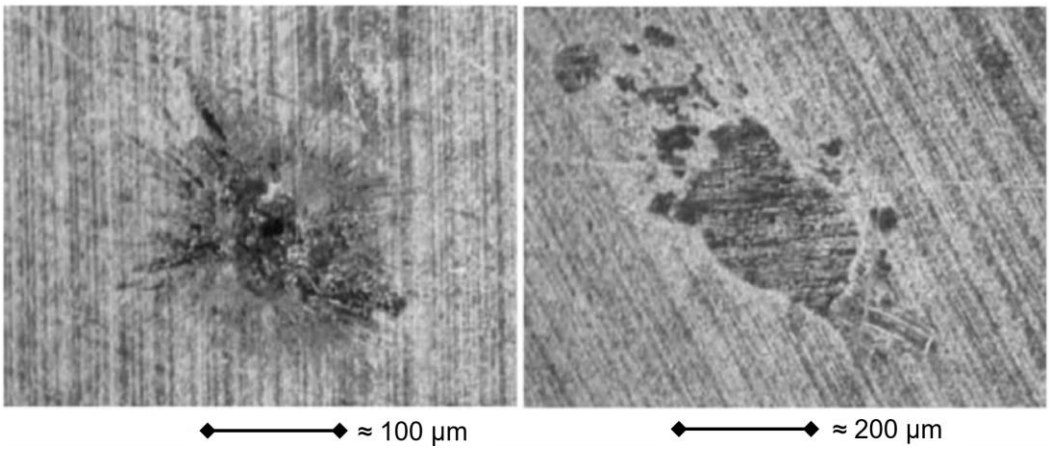

Figure 3. *Picture of cosmic ray destruction in a 4.5 kV diode [3]*

Another example of a cosmic ray failure is shown for a SiC MOSFET in Figure 4. Unlike in Figure 3, the pinhole has a notable size, and the chip seems to be cracked around the pinhole.

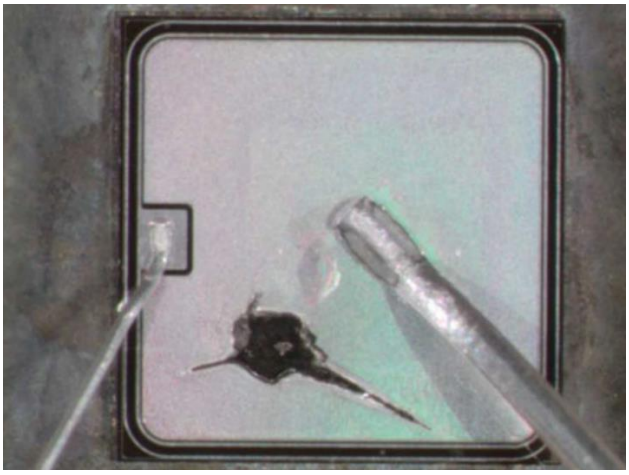

Figure 4. *Cosmic ray failure in a SiC MOSFET [18]*

Regarding the location for the failure in power semiconductors, in [19, 20], finite element (FEM) simulations were concluded to show that for realistic doping profiles the electric field spike in n^-/n^+ junction was higher than the one in p/n^- junction. This means that the impact ionization at the n^-/n^+ junction is a key point for triggering cosmic ray failures in power devices. The higher the field spike in the n^-/n^+ junction is, the lower the linear energy transfer (LET) of a spallation fragment needs to be to cause device failure. Factors affecting the field spikes are the specific device parameters, geometries, and dopant distribution with the applied voltage. [12]

When proceeding to discussion of power MOSFETs and IGBTs, parasitic bipolar transistors come to take place in the cosmic ray failures. In [12] N-MOSFETs were studied, and the triggering of the parasitic NPN-transistor was shown to inject even more electrons than in the impact ionization discussed before. This effect was proposed to be responsible for SEB failures in MOSFETs and IGBTs [21, 22, 23].

One more failure mechanism that has been proposed to be responsible for SEB failures for mainly power MOSFETs and IGBTs is high current and local heating, also known as Joule heating. This is caused by a strong avalanche breakdown or current-induced avalanche (CIA). More of this mechanism can be found in [21, 22, 24, 25].

To conclude from these failure mechanisms, it is not quite clear how to predict the failure mode for each device and further study is needed. Various views exist on the boundary when for example in IGBTs the failure mode changes from avalanche breakdown to bipolar transistor activation [21].

2.2.1 Diode

A diode is the simplest power semiconductor discussed in this thesis. It is an electronic component with two terminals that conducts current in one direction. Diodes are typically used for uncontrolled power rectification in applications such as battery charging and DC power supplies. Regarding cosmic ray-induced failures, diodes have been used for the preliminary study because of their simple structure.

Diode differs from MOSFET and IGBT by not having a parasitic transistor, which tends to get triggered by high-energy neutrons. Even strong local avalanche breakdown, which has been proposed as one failure mechanism, is told to be stable in diodes [3]. This is one reason that gives radiation robustness to diodes.

Some of the first tests for diodes were done in [2] and an exponential failure dependence on the bias voltage was found. Leakage current was monitored during these tests and showed no change before the fault. This means that there is no prior indication of the failure, and it can happen throughout the “normal life” of the device. Thus, cosmic ray failures are acknowledged as random failures and infant mortality or wear-out do not accelerate them.

As mentioned before, cosmic ray robustness is a tradeoff for optimizing the device characteristics. For high-voltage diodes, cosmic ray robustness might be difficult to achieve as it contradicts soft-recovery behavior [3]. Furthermore, design has a remarkable effect on the failure probability, and for example, controlled axial lifetime (CAL) diodes have been proven to be very robust to radiation [4]. One reason for this is the high ruggedness at high commutation speed where dynamic avalanche occurs [26, 27]. For diodes, impact ionization at the n^-/n^+ junction and dynamic avalanche at the p/n^- junction were found to be responsible for the failures. In CAL-diodes, a soft n^-/n^+ junction with increased doping is used and impact ionization in the n^-/n^+ junction is thus shifted to a high current level, increasing radiation stability. [4]

2.2.2 Power MOSFET

Power MOSFETs are controlled power semiconductor devices that are commonly used at high power levels with an isolated gate input. They are especially suitable for high-frequency low voltage applications, such as power supplies, DC-DC converters, and motor drives. They differ from diodes e.g., by being controllable and having the possibility to conduct current in both directions. The structure for a power MOSFET [28] is presented in Figure 5.

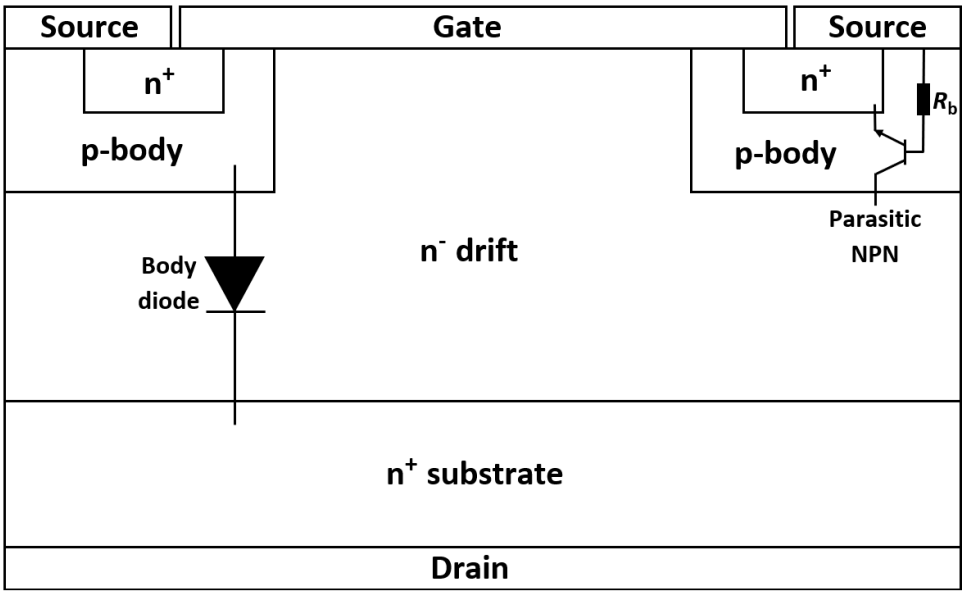

Figure 5. *Structure of a power MOSFET*

Parasitic bipolar NPN-transistor, also shown in Figure 5, has been acknowledged to increase cosmic ray failures [12]. Power MOSFET includes a body diode and the R_b stands for body region spreading resistance.

Unlike diodes, power MOSFETs are acknowledged to be challenging regarding cosmic ray failures. This is mainly because of the already mentioned failure mode, where the parasitic bipolar transistor is triggered. Adjusting the structure of the power MOSFET has been studied for improved radiation robustness and for example in [19] the distance between regions compensated with p-columns and the n^+ substrate was seen to have a positive effect. In addition, the cell structure has been seen to affect the failure probability. [3]

2.2.3 IGBT

Insulated-gate bipolar transistor (IGBT) is a power semiconductor device, that has a control input with a MOS structure and a bipolar transistor that switches the output. IGBTs are designed for high-voltage and high-current applications with low power input e.g. variable-frequency drives, electric cars, and air conditioners. IGBT structure is like a power MOSFET but has the n^+ drain replaced by a p^+ collector layer. This replacement forms a vertical PNP bipolar junction transistor. IGBTs are controlled to switch on and off very rapidly with the help of pulse-width modulation (PWM). The structure of an IGBT [29] is presented in Figure 6.

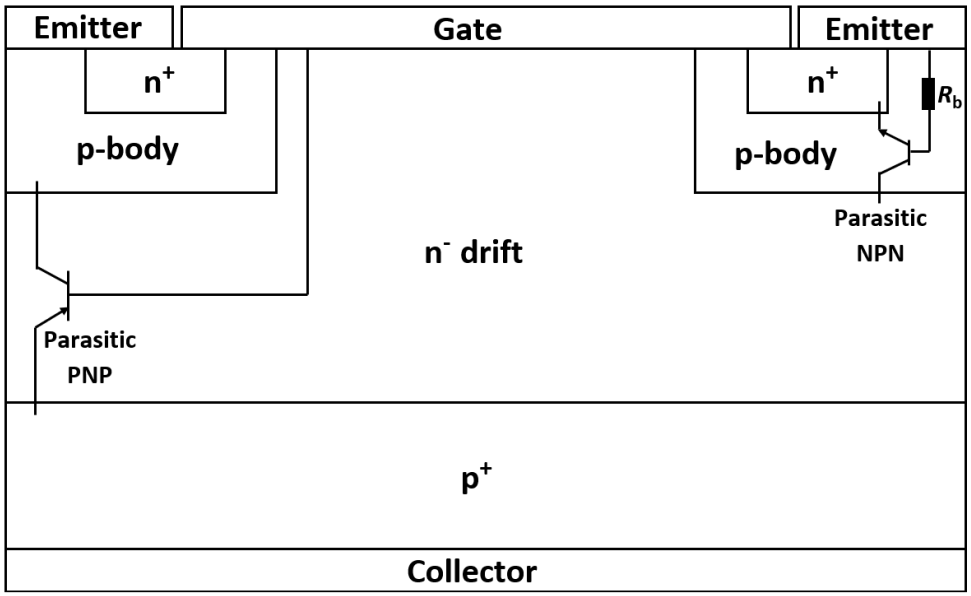

Figure 6. *Structure of an IGBT*

As was the case with power MOSFETs, also in IGBTs one responsible failure mode for cosmic ray failures is the activation of the parasitic NPN-transistor. In addition, in IGBT a parasitic PNP-transistor, that does not exist in a power MOSFET, might activate causing destruction. This theory is supported by simulations presented in [30]. Thus, suppression of the current amplification of parasitic transistors is important when it comes to the improvement of radiation robustness. Parasitic transistor activation is known as destructive latching in IGBTs. [3] In IGBTs, where a buffer layer n^+ is designed between the collector and drift layers, the formation of an Egawa-field between the p/n^- and the n^-/n^+ junctions has been supposed to be involved in the root cause of a cosmic ray failure [20].

Plenty of different IGBT designs have been developed and all of those should be investigated for cosmic ray stability as there are differences among them. In [30] different types of IGBTs were tested and their failure rates as a function of bias voltage were drawn in Figure 7.

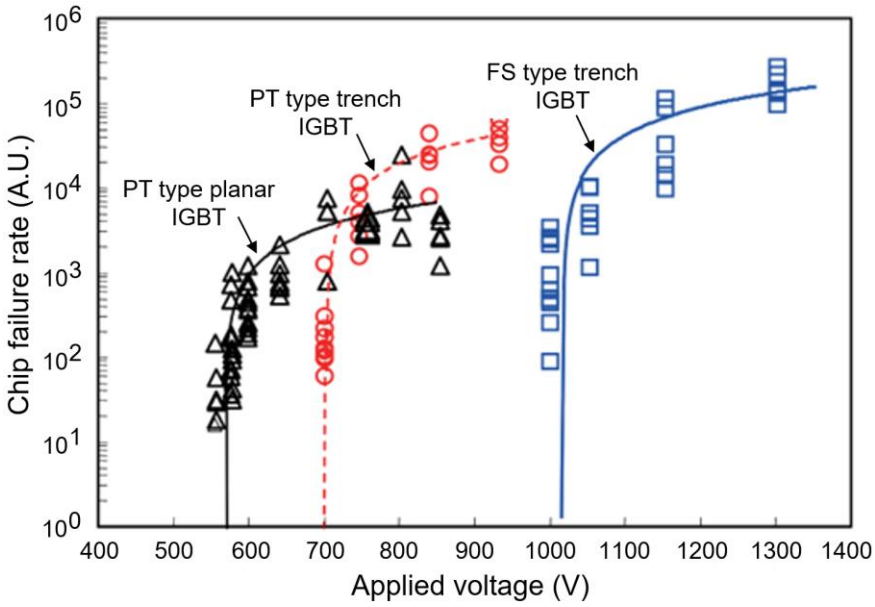

Figure 7. *Different IGBT chips vs applied bias voltage [30]*

These results show that field-stop type IGBT has the highest voltage threshold for SEB. In this same research, it was concluded that the thickness of n^- layer, also known as drift-region, was the dominant factor for radiation robustness. It was also seen that p^+ layer does not have any effect on the FIT rate [21, 30].

2.3 Affecting factors

There are several things to be considered when discussing cosmic ray failure probability. As mentioned previously, neutrons are the main destruction source out of all cosmic particles coming from space. The intensity of these neutrons might vary heavily depending on the location and altitude. As shown in [31], for example, in Colorado there is 13 times higher irradiation intensity than in New York. New York is selected as the reference point and typical failure rates are presented using intensity in this city at sea level. Other factors are blocking state voltage and junction temperature in the power semiconductor device. All these factors are discussed below.

2.3.1 Blocking voltage

The blocking voltage has a major importance in causing cosmic ray failures. The higher the voltage, the higher the probability of failure. Cosmic ray failures for silicon devices start usually occurring at around 2/3 of the rated voltage. When this threshold is reached, the failure rate starts to increase exponentially [32] as we saw in Figure 7. Therefore, the applied voltage to the power semiconductors is typically limited to ~70% of the devices'

rated voltage to ensure high reliability [33, 34]. Results in [35] show the increasing FIT as a function of bias voltage for different power semiconductor devices (Figure 8).

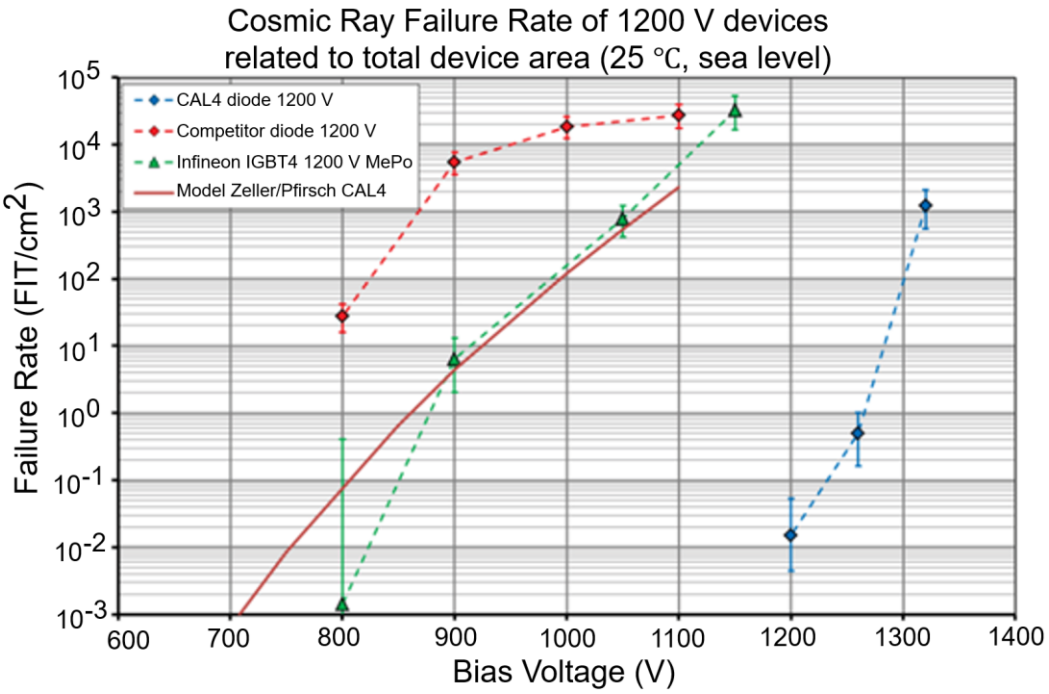

Figure 8. *FIT/chip area vs bias voltage for two types of diodes and an IGBT [35]*

The exponential increase when a certain voltage threshold is achieved in failure rate is visible in Figure 8. This can become a problem when higher voltage applications are to be considered. The typical FIT rate requirement for power modules is <100 FIT, which seems to be surpassed at 825 V for the state-of-the-art competitor diode, 985 V for the IGBT, and 1300 V for the CAL-diode. However, the FIT rates shown in Figure 8 are as FIT/cm^2 and to get a FIT rate for the complete power module, the total area of the chips needs to be calculated. The results show remarkably good robustness of CAL-diodes which was also seen in [4]. These results act as a very good motivator to take different types and designs of power semiconductors into consideration for high-voltage applications to achieve better cosmic ray stability.

Regarding different applications for power semiconductors, the voltage profile should be acknowledged. One example of a typical high-voltage application would be a solar central inverter. This type of application was simulated in [33] and the results showed that most of the time a photovoltaic inverter with maximum DC voltage would have a DC link voltage between 630 V and 750 V but could reach voltage levels up to 820 V at high solar irradiances. The total weighted FIT rate for this type of system would be calculated by multiplying the voltage-dependent FIT/component by the time percentage and the resulting FIT by the number of components. More about this type of voltage profile calculation for different systems and voltage profiles can be found in [33].

The blocking voltage threshold, where cosmic ray failures start to occur, changes depending on the energy of neutrons. This was shown in [36] where tests for over 2000 power transistors were done. Fast neutrons with energies up to 10 MeV caused SEB failures in power devices only at the collector voltage close to the rated values. For example, a 650 V Si power MOSFET started to face SEB failures at 560 V. When ultra-fast neutron (<800 MeV) irradiation was used, the same power MOSFET faced its first failures already at 350 V. When failure rates were calculated, ultra-fast neutrons with very high energies had failure rates several orders of magnitude higher than fast neutrons. [36]

The blocking voltage level can affect which failure mechanism is responsible for a SEB failure. Results from [12] showed that at least for silicon devices with a voltage rating of 600 V, bipolar action is the dominant factor to describe cosmic ray failures. For voltage ratings of 1200 V and above, parasitic bipolar transistors did not influence the failure rates of MOSFETs and IGBTs. This observation leads to an assumption that avalanche breakdown would cause the component breakdown for higher voltage levels.

2.3.2 Junction temperature

Junction temperature is acknowledged to be an effective factor regarding cosmic ray failure rates. The lower the junction temperature, the higher the failure probability. This is because the speed of the charge carriers decreases as the temperature increases. Also, decreasing avalanche ionization rates in higher temperatures are increasing the critical field strength of silicon [3, 4]. Some formulas have been presented to model the temperature dependency for SEB failures. Semiconductor manufacturers prefer to indicate failures at room temperature of 25 °C. With the following formula from [4], for example, if junction temperature T_j is increased to 60 °C and temperature constant T_0 of 47.6 K [5] is used, FIT (λ) will be decreased roughly by half compared to the room temperature. One must keep in mind that T_j needs to be as kelvins in equation (1).

$$\lambda(T_j) = \lambda_0 \cdot \exp\left(-\left(\frac{T_j - 298\ \mathrm{K}}{T_0}\right)\right) \quad (1)$$

Testing of temperature dependency on FIT requires a lab environment where temperature can be varied and kept constant. This was done in [4] by inserting test samples on a hot plate or using a climatic chamber to decrease the temperature down to -40 °C. In these tests it was found that the temperature constant had variation, being 23 K for sample 1 and 56 K for sample 2. The proposed temperature constant of 47.6 K by ABB [5] fits these observations. More tests are planned at the Paul Scherrer Institute (PSI) when an accelerated test setup is available for temperature dependency [4].

2.3.3 Altitude

Altitude is a major factor in cosmic ray failures due to its impact to the neutron flux density. Viktor F. Hess won the Nobel Prize for his work in 1912 when he succeeded in the first measurements of terrestrial cosmic ray densities. He used a balloon to take two ionization chambers up to 5 km altitude and showed the increasing flux density with altitude. Hundreds of measurements were done afterward and in 1936 density detectors were carried high enough to show that after peaking, flux density would decrease at very high altitudes. From these findings, the Pfotzer curve was introduced to show an exponential increase in cosmic rays up to 15 km, above which cosmic rays decreased. [1]

Typically, semiconductor manufacturers introduce failure rates on sea level, but formulas have been presented to calculate FIT in different altitudes. For example, Semikron presents that FIT roughly doubles with a 1000 m altitude increase up to 3000 m [17]. ABB has presented a formula to calculate cosmic ray failures in different altitudes (h), however it will not take device parameters into account [5].

$$\lambda(h) = \lambda_0 \cdot \exp\left(\frac{1-\left(1-\frac{h}{44300}\right)^{5.26}}{0.143}\right) \tag{2}$$

When sea-level altitude is used, h gets a value of zero, and the altitude factor becomes unity. One example of using this formula to calculate temperature dependency on the FIT was done by ABB for a 1700 V HiPak IGBT module [5]. Three different altitudes up to 6000 m were calculated and drawn in a graph presented in Figure 9.

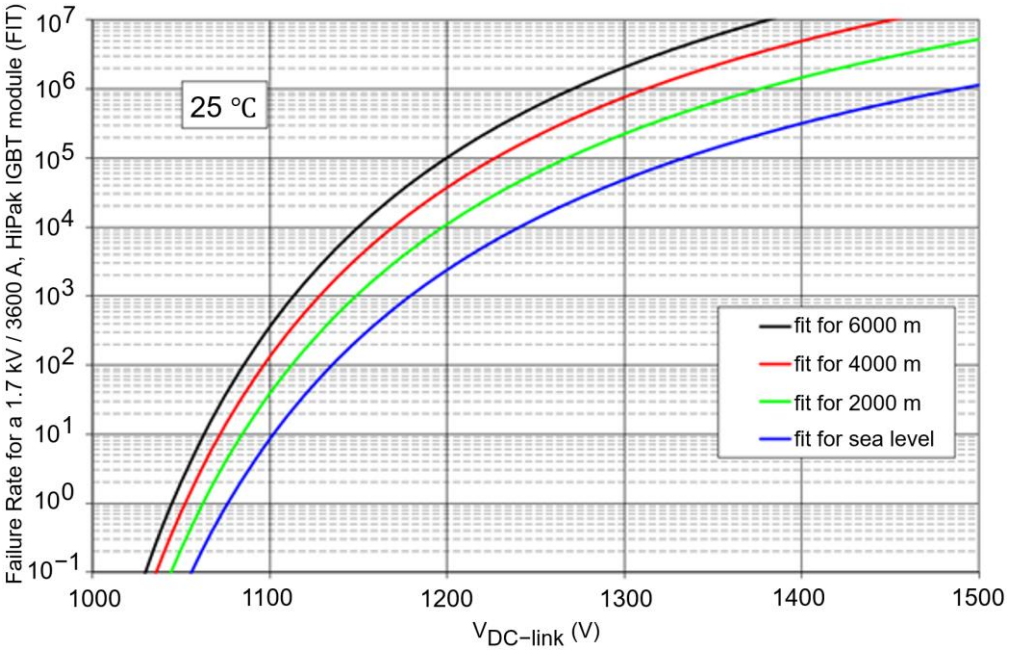

Figure 9. *Altitude vs bias voltage for a 1700V/3600A HiPak IGBT module [5]*

Cosmic ray intensity is claimed to be at its peak at about 10-25 km altitude, which is the typical altitude for airplane flights. These altitudes have intensities about 100 hundred times worse than terrestrial altitudes. However, these altitudes don't have much data as there are only a few results from short airplane and balloon flights. The space environment, on the other hand, has plenty of data to prove very high flux densities from long-term experiments running up to 70 years. [1]

Altitude dependency has been justified by tests at different altitudes. Zugspitze and Jungfraujoch in the Alps are famous places for these tests. In [8] similar tests were done in Zugspitze (2964 m) and Munich (400 m) and an acceleration factor of 8 was found. Nowadays, it is more common to use particle accelerators to accelerate cosmic ray testing even more and to make lower FIT rates possible to measure within reasonable test time.

2.3.4 Radiation flux

Sun was already mentioned as one of the origins of cosmic rays. Sun produces varying solar flares as a function of time and thus the solar particles can have different energies. Sun activity has been measured for decades and it has shown a repetition in about 11 years [37, 38]. During large solar flare periods, the total intensity of terrestrial cosmic rays might double [1].

Even though the sun produces cosmic rays, it can also be thought of as a protector from cosmic rays from outer space. Large solar wind strengthens the magnetic field on earth that acts as a shield against cosmic rays. This shielding effect during active sun periods can reduce terrestrial cosmic rays by about 30 %, however, this reduction is visible with a delay of one to two years. [1, 3] In Figure 10 the solar activity and the terrestrial neutron flux density as a percentage of baseline during the years 1983-2013 in Moscow is presented.

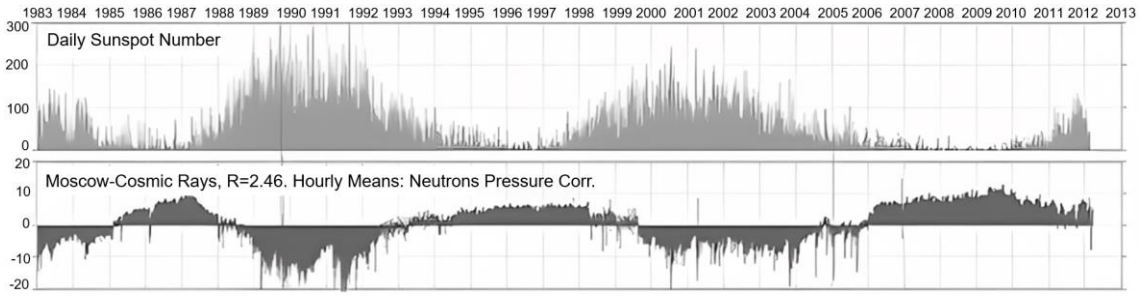

Figure 10. *Sun activity and relative neutron flux on terrestrial altitudes [37]*

Because the magnetic field acts as a shield for cosmic rays, geomagnetic coordinates must be used to calculate and understand the risks of cosmic rays within the whole world. At the equator, the shielding effect is told to be strong and for comparison, at the poles,

the cosmic ray intensity gets three times the intensity of the equator latitude [1, 3]. In [39] the terrestrial nucleon flux was estimated in different cities knowing the geomagnetic coordinates and altitudes. Location influences magnetic rigidity, which means the minimum momentum per unit charge, that a particle must have to reach a location on earth. The higher the rigidity, the less neutron radiation exists at a given location. Results are shown for average solar activity (Table 1).

Table 1. *Neutron flux in different locations compared to New York City (NYC)*

Location	Altitude (m)	Magnetic rigidity (GV)	Relative neutron flux
Bangkok, Thailand	20	17.4	0.52
Berlin, Germany	40	2.8	1.01
Denver, USA	1609	2.8	3.76
Jungfraujoch, Switzerland	3580	4.5	12.8
New York, USA	0	2.08	1
Sidney, Australia	30	4.5	0.92
Vaasa, Finland	6	0.95	1.02

The locations presented in Table 1 have a variety of altitudes and magnetic rigidities which have a significant effect on the relative neutron flux compared to NYC. The calculation for neutron fluxes in different locations is possible because the shape of the neutron energy spectrum above a few MeV does not change significantly with altitude, latitude, or solar modulation. The relative neutron flux could be accounted for in the failure rate calculations especially when power semiconductors are operated at locations with a significant neutron flux difference compared to NYC. More instructions on this type of calculation can be found in [39, 40].

3. QUANTIFYING COSMIC RAY FAILURES

Especially in the early stages of the development of power semiconductor modules, it is utterly important that cosmic ray robustness can be predicted. For the very first radiation robustness predictions, empirical calculation models have been developed to give some direction. However, these models can give results that differ from reality as will be shown below. To give more precise estimations, simulation models including semiconductor type and parameters have been developed and are constantly being improved. One more aspect of failure rate calculation is the operating conditions, such as voltage profile, temperature, and neutron flux. This was already discussed in Chapter 2.3 but it should be mentioned that most likely these factors are difficult to estimate when multiple different end customers and applications exist for the product.

3.1 Empirical models

Empirical models are the most cost-effective and time-efficient way to model cosmic ray failure rates. Empirical models are based only on the initial state of the power semiconductor i.e., geometry, applied bias voltage, and electric field distribution in the device. As told before, impact ionization is a prerequisite for cosmic ray failure and the electric field will be of primary importance for such an approach. [12]

3.1.1 Zeller model

A model to describe failure rates of high voltage power semiconductors (>2000 V) based exclusively on the electric field was presented in [7]. In this so-called Zeller model, the failure rate is expressed as the volume integral of a local failure rate density, which in this case depends on the electric field. The Zeller model proved to be successful to describe voltage-dependent failure rates for high-voltage power semiconductors but did not apply to all voltage classes, down to 600 V. [12]

In the Zeller model, there are two main assumptions, the first being the total failure rate of the device being a combination of failure rates of different parts of the device, indicating a linearly independent process. The second assumption is that the failure rate depends only on the electric field. These two assumptions can be concluded by the following formula

$$P_{\mathrm{f}} = \int_{\Omega} P_{\mathrm{lf}}(E)\mathrm{d}\Omega \tag{3}$$

where P_f is the total device failure rate, local device section failure rate P_{lf}, electric field E, and device volume Ω. [41]

For a 1-D device, the differential volume is area A times dx. With an assumption that the electrostatic potential within the device volume varies slowly, dΩ can be written as: $A \times (\mathrm{d}x/\mathrm{d}E) \times \mathrm{d}E$. In addition, using the Poisson equation, (dx/dE) can be replaced by ε/ρ, where ε is permittivity and ρ is net charge density. With these modifications, the previous formula for total device failure rate transfers to

$$P_f = A \times \epsilon/\rho \times \int_{\Omega} P_{lf}(E)\mathrm{d}E. \quad (4)$$

This indicates that the total cosmic ray failure rate is a function of drift region doping, which defines the ρ and E within the active device volume. It is told that in a non-punch through (NPT) device, electric field lines terminate in the drift layer and this field is proportional to the square root of the product of the drift doping and applied voltage. For a punch-through (PT) device, [7] describes the dependence of the electric field on drift doping and applied field changes. [41]

In [4] the Zeller model is found to predict the failure rate of a 1700 V CAL-diode quite well in a voltage range over 1500 V because every streamer leads to destruction. When the voltage range decreases below 1500 V, not every streamer is destructive and the prediction from the Zeller model exceeds the realistic failure rates. The position of this cut-off [9] for destructive streamers depends on the doping profile at the n^-/n^+ -junction. The doping profile is not part of the Zeller model and therefore it cannot predict the cut-off voltage range. However, with identical cathode doping profiles, the cut-off voltage has been proven to be independent of the voltage level of the power semiconductor device. [4]

3.1.2 Pfirsch model

In [6], another model called the Pfirsch model, is proposed and differs from the Zeller model by acknowledging the local failure rate density as a function of spatially averaged electric field E_{av} and applied direct current voltage V_{DC}. The Pfirsch model presents a voltage-dependent correction factor f(V_{DC}) to better match the calculated FIT rates to experimental FIT rates. The Pfirsch model corresponds to Chynoweth law for impact ionization and is defined as follows

$$\lambda = f(V_{DC}) \cdot a \cdot \exp\left(-\frac{b}{E_{av}}\right) \quad (5)$$

where a and b are parameters that were introduced in [6].

For >2 kV devices f(V_{DC}) equals one and for <500 V devices the correction factor gets so low values that the FIT rate becomes insignificant. The Pfirsch model results for devices rated from 600 V to 6.5 kV were compared to experimental results in [6] and are shown in Figure 11.

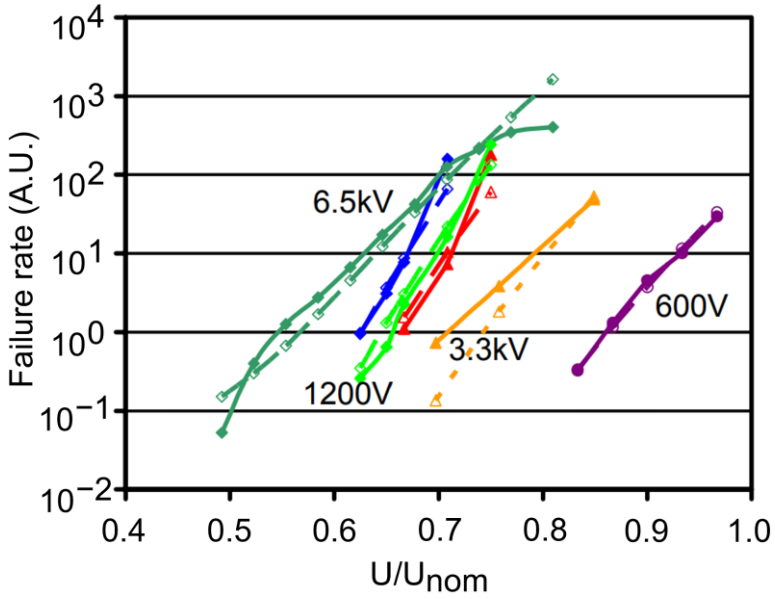

Figure 11. *Comparison of failure rates calculated with the Pfirsch model (dashed lines) and experimental results (full lines) for different diodes [6]*

The comparison seems to have a good match with the calculations and the experimental results. The correction factor has a positive effect on the accuracy of the FIT calculation, especially in the lower voltage regions. More about the Pfirsch calculation method can be found in [6].

3.1.3 Kaminski model

The third model is Kaminski's model which has been developed based on experimental results from IGBT power modules of ABB. The Kaminski model differs from Zeller and Pfirsch by taking temperature and altitude into account. The full Kaminski model was presented in [5] and is written as follows

$$\lambda(V_{DC}, T_j, h) = C_3 \cdot \exp\left(\frac{C_2}{C_1 - V_{DC}}\right) \cdot \exp\left(\frac{25 - T_j}{47.6}\right) \cdot \exp\left(\frac{1 - \left(1 - \frac{h}{44300}\right)^{5.26}}{0.143}\right) \quad (6)$$

where $V_{DC} > C_1$. This means that the formula cannot be used to calculate FIT rates for voltages under a certain value. This should not raise a lot of concern because low voltage gives low failure rates and are not critical from the quality point of view. Temperature (now in Celsius) and altitude factors were already presented in chapters 2.3.2 and 2.3.3

but voltage factor contains device-specific parameters C_1, C_2, and C_3 which can be looked up from a table presented in [5].

The voltage dependency cannot be used for power semiconductors from other manufacturers than ABB as it requires device-specific parameters from ABB. The temperature and altitude dependency, however, seems to match with failure rates estimated by some power semiconductor manufacturers. This comparison indicates that the altitude and temperature factors are considered accurate for estimating failure rates in different environments.

3.1.4 Model comparison

The Zeller model was first published in the 1990's being the first empirical model for cosmic ray failure rate prediction. It took only the electric field into account and gave accurate results for semiconductor devices operating at high voltage levels. The Pfirsch model was then published in 2010 taking the electric field and the blocking voltage into account and giving more accurate results compared to Zeller, especially for lower voltages. The Kaminski model is different from these two models and was developed based on experimental data from ABB's IGBT power modules. However, for the sake of comparison in [3] the failure rate as a function of applied bias voltage for a 1700 V power semiconductor was calculated using these three methods (Figure 12).

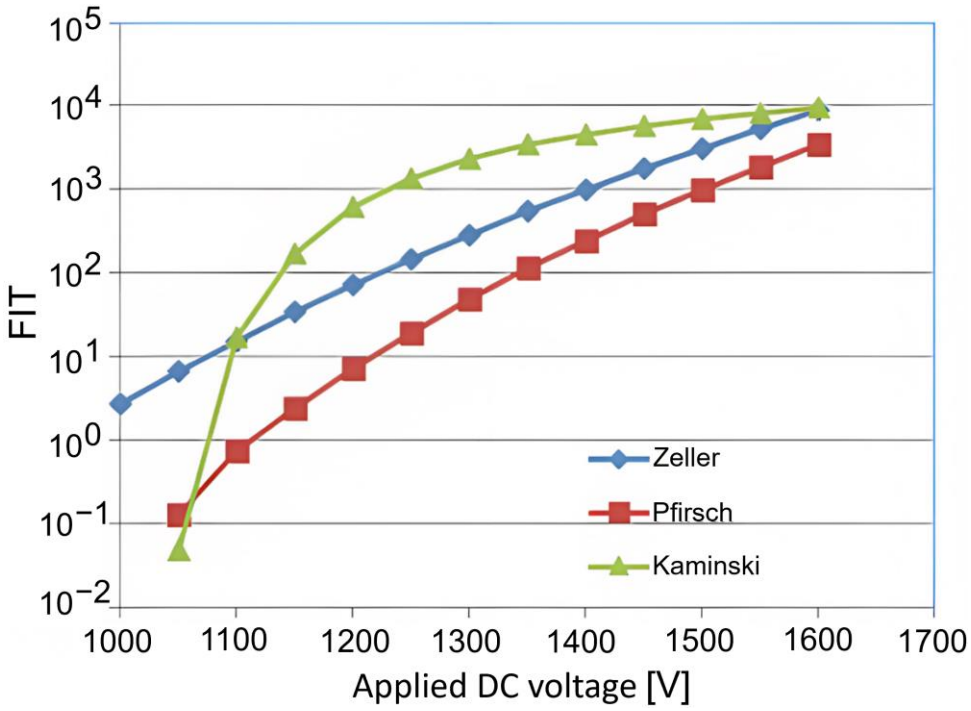

Figure 12. *Failure rate comparison for a 1700 V power semiconductor using three different empirical models [3]*

The Pfirsch model seems to predict the lowest failure rate almost in the whole considered voltage range. The Zeller model gives a higher failure rate estimate but has the same shape for the prediction curve as Pfirsch. The Kaminski model predicts the highest failure rate and has a completely different shape of the curve with a very high increase at voltages 1050-1200 V after which the failure rate seems to saturate. Overall, the difference between these prediction methods is high and indicates the error that can result from calculating FIT rates with these models. The results of the highest and lowest failure rates, depending on the selected calculation model, are almost two decades from each other. This indicates the high need for experimental tests to reduce uncertainty.

3.2 Simulation

The target of power semiconductor simulation is to point out designs that should improve the radiation hardness. Now, these simulation models do not offer the possibility to calculate absolute failure rates but are a very beneficial tool to help with designing power semiconductor properties i.e., n^-/n^+ -junction thicknesses. To make working simulation models, the mechanisms that lead to cosmic ray failures, from initial charge deposition to the evolution of electric fields, charge densities, currents, heat generation, and temperature rises need to be understood. [12]

A common simulation tool for modeling cosmic radiation robustness for power semiconductors is Technology Computer-Aided Design (TCAD) by Synopsys. This tool includes a heavy ion model that has been used in many studies [21, 25, 32, 42, 43] because it has been proven to give results in good agreement with experimental results [25, 43]. In this heavy-ion model, high-energy particles transfer energy to the atoms and generate electron-hole pairs as they pass through the device in a blocking state. In the model, cosmic ray failure is attributed to collector current runaway. [32]

For power semiconductors, Monte Carlo simulation techniques can be used to generate a spectrum of particles from the interaction of terrestrial cosmic rays with the base material. This spectrum can then be combined with the analysis of existing heavy-ion SEB data for power MOSFETs at low LET and the calculation of sensitive volume from TCAD to estimate the SEB cross section and calculate FIT rates. This is an approach that gives results that agree with experimental data on cosmic ray-induced failures in both ground-level and aerospace applications. [42]

4. TESTING FOR COSMIC RAY FAILURES

Testing for cosmic ray failures is of major importance within power semiconductors for reliability, which can be measured by failure rates. The best way to test for cosmic ray failures would be to test devices under natural terrestrial radiation with different operating parameters. However, this approach has some major issues. The first issue would be the high-reliability targets for power semiconductors ranging from 0.01 FIT/device to 100 FIT/device depending on the application. FIT means one failure in 10^9 operating hours. Testing this kind of failure rate for one set of operating parameters with ten fails on average would require 1000 devices to be operated for 10^7 hours or over 1000 years, which is not feasible in any way. Therefore, storage tests with natural radiation are limited to test failure rates up to several thousands of FIT and for lower failure rates, accelerated testing is used. Another problem is regarding the bias voltage under realistic field conditions, which leads to the question of static bias compared to dynamic. [4, 12]

Accelerated tests with particle accelerators are the most feasible way to reduce test time and allow the measurement of cosmic ray FIT rates at lower voltages. However, it is recommended to compare the results between accelerated tests and tests implemented with natural cosmic radiation. This type of comparison was succeeded in the lab at Semikron in Nuremberg [4]. This lab also could test the previously discussed temperature dependence because the ambient temperature was possible to be adjusted. Also, a test setup for Danfoss Drives at Vaasa was developed in this thesis and will be presented below.

At the time being, there is no standard for determining failure rates caused by terrestrial cosmic rays for power semiconductors. However, for integrated circuits (ICs) there is the JESD89A standard [39] containing some useful information that can be utilized. This is probably because the device development is proceeding at a rapid speed with the goal of loss reduction and increasing current densities. On the other hand, these goals lead to increased electrical field strengths leading to a reduction of cosmic ray robustness. In the past, this has been a problem only for high-voltage high-reliability systems but during recent years, SEB failures have been detected also for voltage levels down to 600 V. This is problematic because of the need for renewable energy systems, such as wind- and solar power with voltage levels of 600-1700 V, has increased. Also, hybrid electric vehicles with very demanding reliability requirements have brought cosmic ray stability under heavy research in recent years. [12]

Not much general experimental data exists in public. Typically, large power semiconductor customers receive confidential cosmic ray FIT curves under the condition of a non-disclosure agreement from power semiconductor manufacturers. This makes an open comparison between different chip designs difficult. However, some researchers have made this kind of comparison for both Si and SiC devices and have brought some insight into this subject [11].

4.1 Storage tests

Storage tests are tests implemented under the natural flux of terrestrial neutrons. The only way to accelerate this kind of testing is by reducing the junction temperature or doing tests in higher altitudes, where neutron flux is increased. Altitude dependencies in different cities and altitudes were analytically expressed in [31, 39]. First accelerated storage tests for cosmic ray failures were done on the Zugspitze (2964 m) [8] and the Jungfraujoch (3580 m) [9]. These tests gave acceleration factors of 11 and 16 which made FIT rates of 1000 per device feasible to measure. While these high failure rates are not used to qualify any devices, it is still in the range of extreme biasing conditions in some applications. Also, it is important to see how natural cosmic rays affect the power of semiconductor devices giving ground to accelerated testing with artificial particle accelerators. Furthermore, storage tests should always be compared to tests with artificial sources to verify results. One more mention to make for storage tests is that more particles of different types are present in the natural environment (Figure 1) and nucleons with energies above 1 GeV are included unlike in an artificial nucleon source. A picture of the measurement hut at Zugspitze for cosmic radiation is shown in Figure 13.

Figure 13. *Measurement hut at Zugspitze for cosmic radiation*

A Timepix3 particle detector locates inside the hut and measures various particles and their trajectories in real-time. It was installed by The German Aerospace Center in cooperation with the universities of Augsburg and Prague. Timepix3 was originally created to measure particles at acceleration facilities at CERN. [45]

4.2 Accelerated testing

When power semiconductors reach the production stage in the development process, accelerated tests using nucleon beam irradiation are to be done to verify the prior simulation results regarding cosmic ray stability. Different design and technology variations are of interest as they identify how easily the device will fail. The importance of accelerated testing is substantial at this point of product development as complete data sets of FIT vs bias voltage must be acquired to optimize the thermal and electrical performance of a power semiconductor by not sacrificing too much cosmic ray robustness. Also, before the product goes to mass production, qualification needs to be done concerning the radiation hardness. This requires close cooperation with the system-level engineers and the device manufacturer. In general, the importance of cosmic ray robustness is well acknowledged, at least for high-reliability high-power system engineers. However, not in every power system has it previously been seen as a problem and more information has still to be shared. [12]

Acceleration of measurement can be achieved by increasing the flux of highly energetic neutrons [8]. However, the interaction of protons with silicon was experimentally and theoretically shown to be equivalent to those of neutrons, as their electrostatic interaction with the silicon nucleus can be neglected [46]. Therefore, protons can be used in place of neutrons in accelerated testing.

A research center in Switzerland, PSI, operates one proton irradiation facility that provides acceleration factors of more than 10^{10}. This makes failure rates below 1 FIT possible to measure with a reasonable number of samples and test duration (Figure 14). Tests succeeded at the PSI in [4] had proton energy set to 200 MeV and flux density varying between 5.4×10^{4} and 3.5×10^{7} p/s/cm^2. This corresponds to an acceleration factor of 1.9×10^{7}-1.3×10^{10} assuming the sea level cosmic ray intensity to be 10 p/h/cm^2. [4]

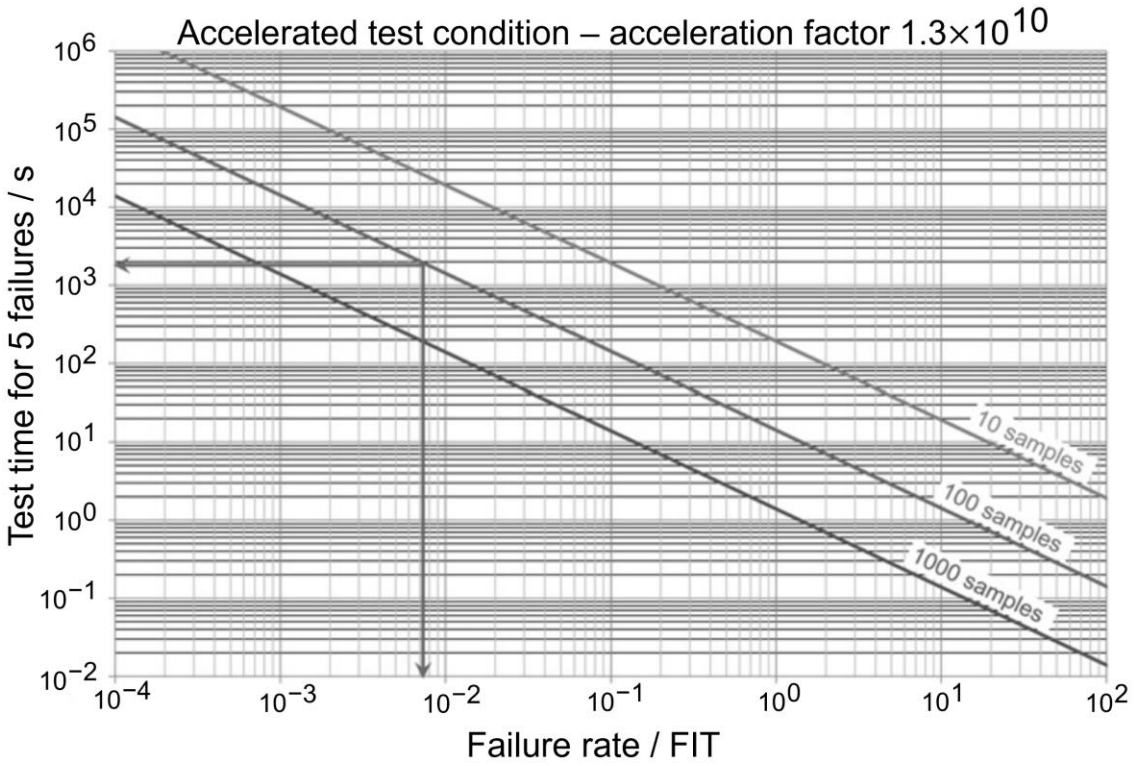

Figure 14. *Average test time to obtain five failures at a specific failure rate for different sample sizes with an acceleration factor of 1.3·10[10]. Practical detection limit for 100 samples marked with arrows. [4]*

The evaluation of failure rate λ implies the detection and counting of the number r of failures of devices under test (DUTs) and registering the number of device-fluence product T_{SUM}

$$T_{\mathrm{SUM}} = \sum n(t_i)\Delta f_i \tag{7}$$

giving a sum over failure events i, with $n(t_i)$ the number of devices at the time of fail t_i and the fluence-to-fail Δf_i. The failure rate is then given by

$$\lambda = r/T_{\mathrm{SUM}} \tag{8}$$

Test results should always have a margin of error to acknowledge. As cosmic ray failures are random failures, the failure rate can be assumed to be constant. In [12] with constant FIT assumption, a formula is presented to find confidence levels

$$(2T_{\mathrm{SUM}})^{-1}X^2_{\alpha/2}(2r) < (2T_{\mathrm{SUM}})^{-1}X^2_{1-\alpha/2}(2r) \tag{9}$$

where X^2 is the chi-square function with $2r$ degrees of freedom and $\alpha = 5\%$ is used for the confidence of 95 %. For different stress scenarios, ten failures are considered reasonable and would give a confidence factor of two. The number of failures in tests can be adjusted by changing the applied bias voltage, temperature, number and area of test devices, intensity of nucleon flux, and time of irradiation. [12]

An example of applying confidence levels to failure rate calculation over experimental data is presented in Figure 15. Mean time to failure (MTTF) shown in the statistics table is in this case calculated using exponential life distribution that generally fits constant failures quite well and is equivalent to 10^9 divided by FIT.

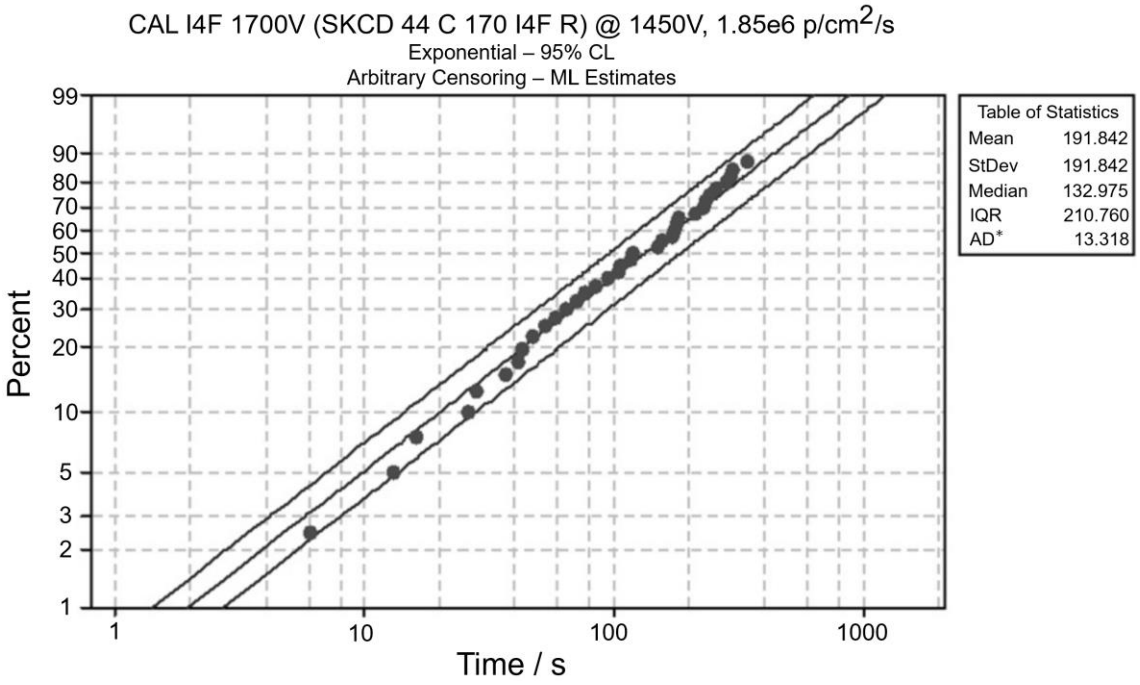

Figure 15. *Experimental data with a 95 % confidence level for a 1700 V CAL diode [4]*

Different artificial nucleon sources exist and some of them have been presented in [47]. These include neutron spallation sources ranging from energies of 70-800 MeV which fit well to the 50-200 MeV spectrum that was one presented origin for most of the SEB failures in chapter 2.2. Also, it was found in [12] that nucleon sources with mono-energetic particles with energies no less than 150 MeV are an appropriate choice for artificially accelerated testing.

One important thing to consider regarding the different types of radiation sources is that these can give different results for the same DUT. This aspect was investigated in [12] and three types of radiation sources, an 800 MeV and a 180 MeV neutron spallation source, and a 180 MeV monoenergetic proton source were compared using a 1200 V IGBT-module as the DUT. The tests concluded the results to end up within a maximum factor of four from each other. This gives a good perspective on the importance of the selected irradiation source, however, researchers behind these tests claim that a nucleon source with energies over 100 MeV would be a good measure for SEB failures.

4.2.1 Dynamic biasing

An interesting observation was made in [4] where accelerated tests were compared to extended tests for several months. Time-consuming tests led to additional failures, that did not occur evenly in chips but occurred near the edges of the chips. These additional failures were explained to be caused by the constant high voltage stress. This kind of voltage stress is not typical for power device applications. When e.g., in the voltage source inverter the active device in the upper branch is conducting the lower branch is turned off. This means that always one of the devices is blocking almost the full DC-link voltage. When the inverter is not running, both devices are turned off and they block only 50 % of the DC-link voltage. This 50-50 split for the blocking voltage is done with a simplifying assumption that no leakage current occurs but in a more realistic approach, blocking voltage would roughly lead to a voltage distribution of 60 to 40 %. Furthermore, the nominal DC-link voltage must be lower than the rated blocking voltage to take overvoltage during switching into account. It is preferred to include these overvoltage surges during cyclical voltage stress in the SEB failure rate calculation giving a voltage weighting factor depending on the application profiles [12]. As a conclusion, cyclical voltage stress would be a more realistic test condition for cosmic ray robustness. [4]

In [4] a 50 Hz square wave voltage with a 50 % duty cycle was used to check whether the additional failures caused by constant voltage would disappear. Test time was doubled but the results, in this case, had a better match to the accelerated tests. This confirmed the suggested constant high voltage stress to cause additional failures.

Research on the influence of dynamic switching also succeeded in [48] for 6.5 kV IGBTs and freewheeling diodes (FWDs). Different bias conditions and switching rates were addressed by synchronizing IGBT switching to the extraction frequency of a proton beam from a synchrotron. The extraction frequency gave a time window of 30 µs for a pulse with an overvoltage peak of the reverse recovery, which is relatively low for a 6.5 kV IGBT and thus allows the separating of failures due to switching from those due to static voltage. In these tests, a significant increase of 20-40 % in cosmic ray failures was found because of the dynamic bias voltage. Also, simulations with semi-empirical models, which were discussed in chapter 3.1, were in good agreement with the findings in these tests (Figure 16).

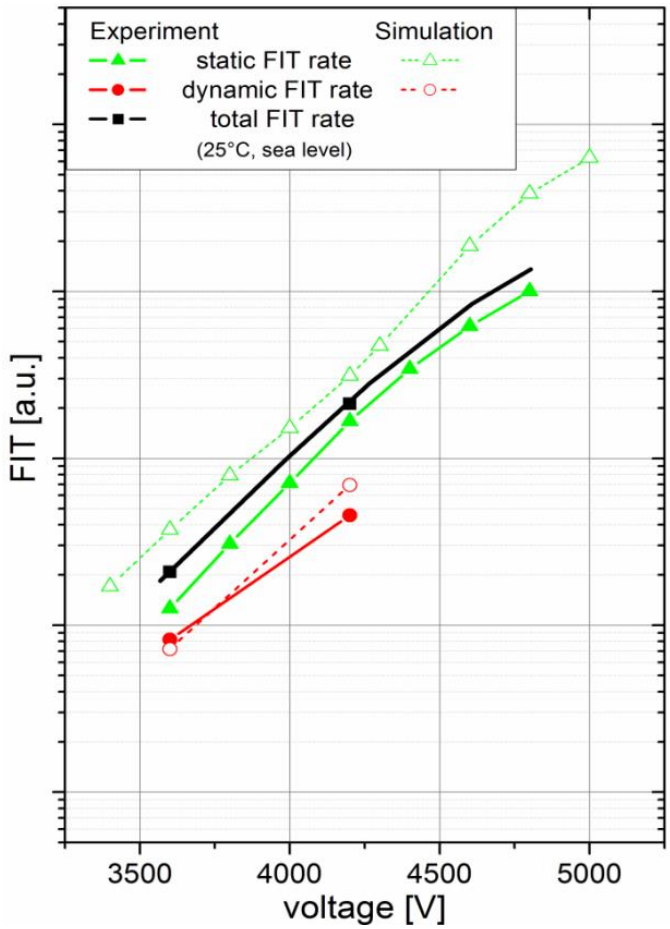

Figure 16. *Failure rates for dynamic and static bias voltages for 6.5 kV IGBTs. Experimental and simulation results are included. [48]*

These results show the dominance of the static FIT rate in the total FIT rate but also indicate the importance of dynamic biasing. This gives great support to the idea of dynamic biasing being a non-negligible factor when radiation robustness is concerned.

4.2.2 Test setups

As mentioned earlier, the selection of an artificial nucleon flux source is important as it can give different results for measured cosmic ray failure rates. Some of the research centers providing these irradiation test setups are presented below.

Los Alamos Neutron Science Center (LANSCE) is maybe the most known research center for cosmic ray failure testing. It has several experimental facilities that can be used for radiation effect research. For example, in [11] tests were done at LANSCE to speed up the measurement process as LANSCE was told to produce neutron flux levels up to 10^9 times the New York sea level flux. The radiation effects of three different neutron sources at LANSCE [10]: ICE-II, Thermal neutrons FP 8, and East Port are shown in Figure 17.

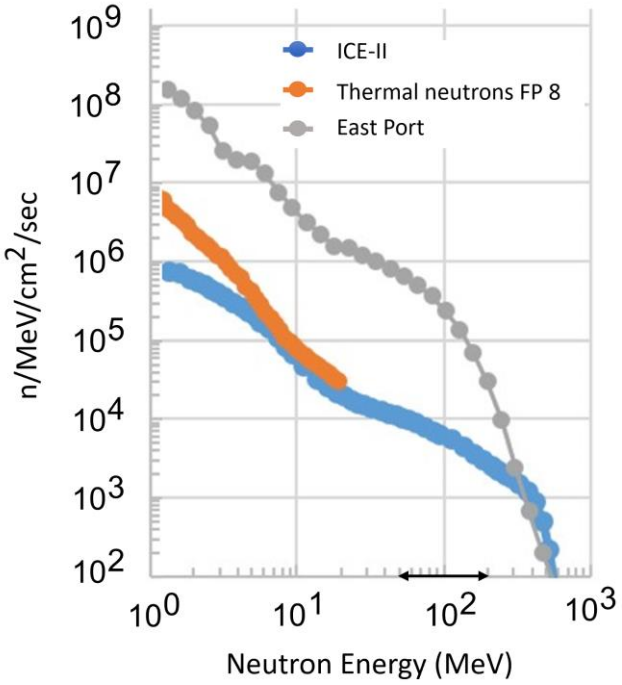

Figure 17. *The shape of the neutron spectrum at LANSCE, 1-1000 MeV*

Regarding cosmic ray failures in power semiconductors, referring to the previous discussion in this thesis, the interesting neutron energies 50-200 MeV are marked in Figure 17. Moreover, by looking at the Figure 17, suitable neutron sources for failure rate testing at these energies would be ICE-II and East Port as Thermal neutrons FP 8 does not reach energies over 20 MeV.

LANSCE claims that the ICE-II neutron spectrum is very similar to the terrestrial neutron spectrum produced by cosmic rays and ranges from 1 MeV to 600 MeV. The integrated neutron flux intensity for energies above 1 MeV in this accelerator is approximately 5×10^6 neutrons/cm^2/sec. Many industries, laboratories, and university researchers have used ICE-II to test cosmic ray stability for semiconductors. The other suitable neutron source, East Port with integrated neutron flux from 1 MeV to 600 MeV of 6×10^9 neutrons/cm^2/sec, is told to be used mostly for material irradiation effect research. [10]

The spectrum for neutron fields at LANSCE ICE House has been compared to the spectrum determined at Jungfraujoch in [49]. The comparison is presented in Figure 18 for flux per lethargy, which represents equal energy-integral fluxes of equal areas under the spectrum of different energy regions [39].

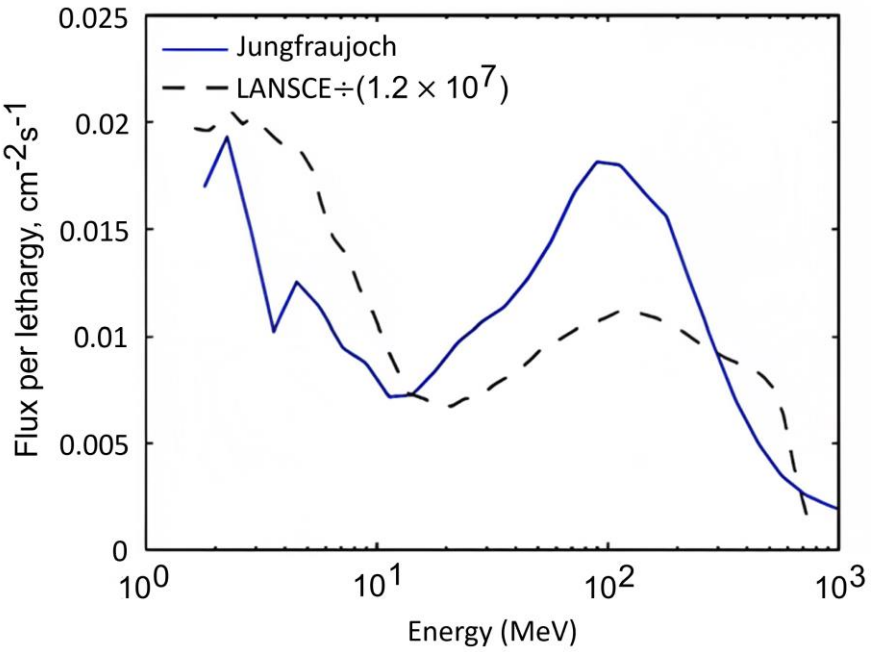

Figure 18. *The neutron flux per lethargy spectrum determined at LANSCE and Jungfraujoch [49]*

The spectrum at Jungfraujoch was determined by the Qinetic Atmospheric Radiation Model (QARM) [50] which considers factors such as date, large-scale solar modulation of primary rays, and a planetary index to account for solar influence on the earth's magnetic field. The results from QARM simulations for the neutron spectrum at Jungfraujoch seem to be quite similar to the LANSCE Ice House spectrum. However, the neutron flux below energies of 10 MeV is lower at Jungfraujoch and for higher energies, LANSCE provides lower neutron flux. [xx]

Another known neutron source for semiconductor SEB failure testing is the ChipIr at the ISIS Neutron and Muon Source, located in the United Kingdom at the Rutherford Appleton Laboratory [51]. As was the case with LANSCE, neutron flux up to 10^9 times the NYC sea-level flux is provided at the ChipIr but for a wider energy range of 1-800 MeV.

Continuing the list of test facilities, ANITA (atmospheric-like neutrons from thick target) at the Svedberg Laboratory in Uppsala Sweden [52] started operation in 2009 for accelerated cosmic ray failure testing. The ANITA beam is a spallation neutron source that produces a so-called white spectrum, which resembles the spectrum of neutrons in the atmosphere and at the terrestrial level. Therefore, ANITA is suitable for deducing cosmic ray FIT rates for components and systems. A comparison of ANITA and the previously mentioned test facilities for terrestrial flux is presented in Figure 19. Also, a high-energy irradiation facility at TRIUMF in Canada [53] was included in the comparison.

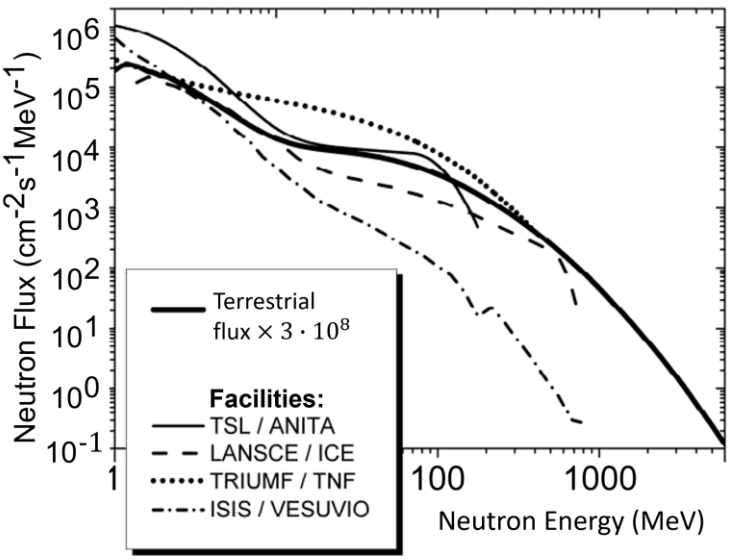

Figure 19. *Comparison of energy spectrums in different test facilities [52]*

As seen in Figure 19, significant differences between neutron beams exist. The best match to terrestrial flux depends on the energy range that is to be examined. At the energy range of 50-200 MeV, ANITA seems to be the most accurate. However, none of these commonly used facilities can claim a perfect similarity to the terrestrial spectrum. Also, higher energies are not reachable with artificial sources.

4.3 Vaasa test setup

At Danfoss Drives in Vaasa, the need for own testing for cosmic ray failures was recognized. The setup developed in this thesis is the first step for this type of testing at Danfoss Drives. The verification of failure rates given by power semiconductor manufacturer A was considered a good approach for cosmic ray failure testing. With natural terrestrial neutron flux, the verification of low FIT rates would not be feasible as the test time would be too high. Thus, the verification of high FIT rates up to hundreds of thousands was considered suitable. This is possible by using a high bias voltage close to the rated voltage of the DUT.

FIT corresponds to one failure in billion hours. For example, 200 000 FIT would correspond to one failure within 5 000 hours. Adding more DUTs to the test setup reduces the required test time. For example, 24 DUTs would reduce the required operating time to nine days. However, when reliability is discussed, a margin of statistical error due to the amount of DUTs needs to be considered. A confidence level and reliability of 90% were considered accurate enough for planning the number of DUTs in the test to see failures in a feasible time frame. Using the Weibull++ test setup planning tool and accounting for the number of DUTs, the required test time increases from nine days to 14 days. This

was considered the first goal of the test setup, but the test is aimed to be continued for multiple months.

An ambient temperature of 25 °C was selected for the test environment. This matches the temperature used in the estimates done by power semiconductor manufacturers. As there is only a very small leakage current going through the chips in this test, no significant heat is generated, and the junction temperature of the chips can be considered to match the ambient temperature. A heater controlled by a proportional–integral–derivative (PID) controller was used to maintain a stable temperature. The temperature was measured throughout the test every ten minutes so the failure rates can be corrected using the formula (1).

The test setup was built inside an isolated trailer van with thin walls consisting of fiberglass and styrofoam. The attenuation of neutrons by the walls of the van was considered insignificant according to data in [54] and the findings in [6]. The foreseen problem with this setup can appear during the winter when snow gathers on top of the van. The snow would block radiation to some extent because hydrogen is known as an effective neutron attenuator according to [54]. Also, discussions with the personnel at Cosmic Ray Station of the University of Oulu [38], located in Sodankylä, confirmed this. More about the shielding for neutrons is discussed in Chapter 5.

The intensity of the neutron flux was estimated in Vaasa using a tool presented in the JESD89A standard [39]. The coordinates and elevation in Vaasa were included in the estimation and for the solar modulation index, the default value was used as suggested by JESD89A. If the location should be at high altitudes and the most accurate value is desired, then the solar modulation index could be approximated e.g., from the measurement data at the Oulu Cosmic Ray Station [38]. The neutron flux in Vaasa resulted to be 2% higher than the reference flux in NYC. The difference was chosen to be ignored in the FIT calculation as it is very small and the data from [38] shows that the solar modulation should be below the default value, and this would decrease the neutron flux at Vaasa.

The first tests had 24 samples of 1200 V IGBT power modules connected parallel with a high-voltage DC power. A constant test voltage close to the rated V_{CE} was selected. Gate-emitters of both the top and the bot branches in the tested power semiconductors were shorted to assure a constant blocking state. To allow comparison between the 50 % duty cycle estimate by the component manufacturer, only top branches were connected to the DC power. 50 mA fuses were connected in series with the output terminals of DUTs while the current limit of the DC power was set to 100 mA. The fuses isolate the

broken devices from the test circuit and the test can continue without the removal of the broken DUT. The principle of the test setup is presented in Figure 20.

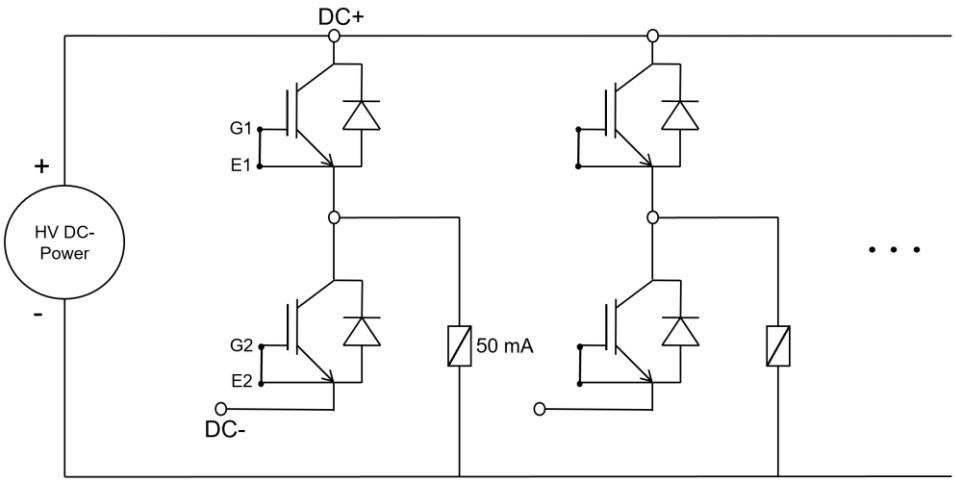

Figure 20. *The principle of the cosmic ray test setup at Vaasa*

The resistance of the fuses is measured daily to indicate the time to failure. The circuit is disconnected from the supply during these measurements and the voltage is slowly ramped back to the target after the measurement. The simple structure of the setup is seen as a benefit in the failure analysis. However, constant high voltage has been seen to cause additional failures and cyclical voltage stress has been noted to give more realistic failure rates at the system level [4, 35, 48].

4.3.1 Results

After two months of testing, six failures have occurred. The tests continue with 18 modules and as the number of DUTs reduces, the expected time to failure increases. The first failure was seen on a diode and the second on an IGBT (Figure 21).

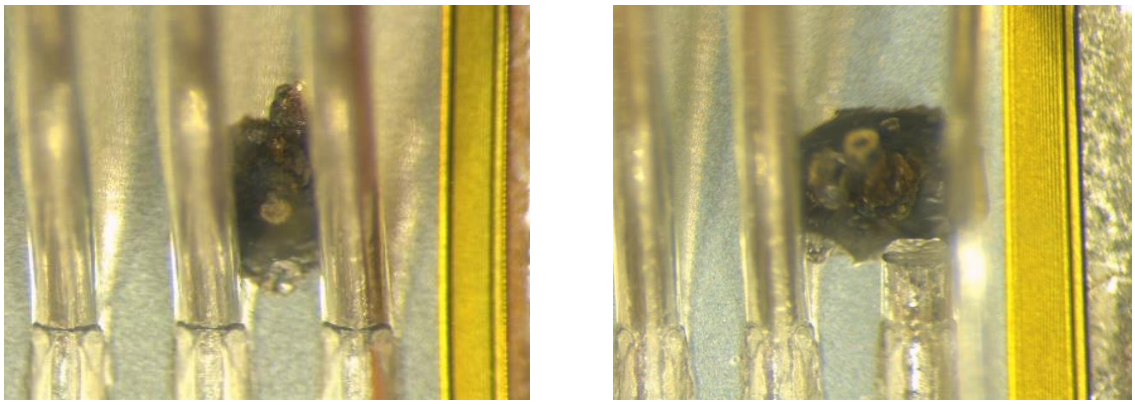

Figure 21. *The first failure (diode) is on the left, and the second failure (IGBT) is on the right*

The third and fourth failures occurred on IGBTs (Figure 22).

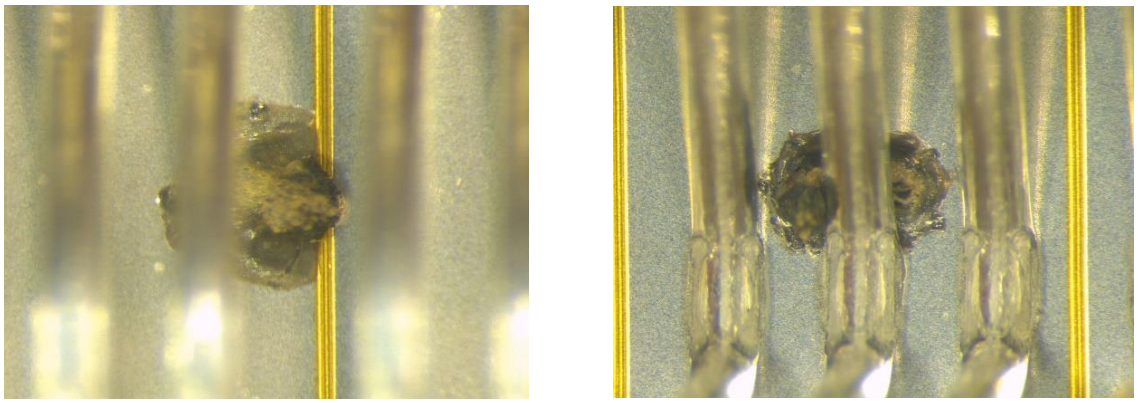

Figure 22. *The third failure is on the left, and the fourth is on the right. Both failures on an IGBT.*

The fifth failure occurred on a diode and the sixth failure on an IGBT (Figure 23).

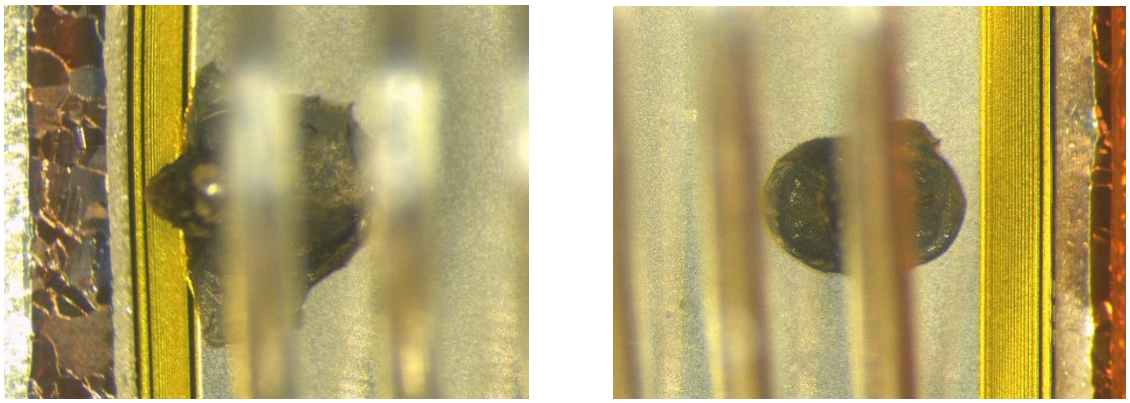

Figure 23. *The fifth failure (diode) is on the left, and the sixth failure (IGBT) is on the right*

The failures presented in Figures 21-23 have similar shapes and sizes. Excluding the fifth failure, they are all perfectly located in the active region and indicate a short circuit as the cause of the failure. Unlike others, the fifth failure seems to touch the passive region at the edge of the chip, and it is not quite clear whether the origin of the failure is at the active region. As mentioned in Chapter 2.4.1, constant high voltage was seen to cause additional failures that tend to locate near the edges of the chip [4]. This kind of behavior can be seen in failures one, two, five, and six.

Regarding the size of the destruction, the failures in Figures 21-23 have a diameter between 1-2 mm. This is a lot more than was seen in Figure 3 but could be in a similar range to Figure 4. The size of the failure might be enhanced because of the 50 mA fuses that were used in series with the power semiconductor modules. However, in a similar test setup in [4], 63 mA lead fuses were used. For future testing, fuses with lower current ratings could be considered to minimize the energy during the failure event to see smaller destruction and to make analyzing the failures easier.

From these results, FIT was calculated using ReliaSoft's Weibull++ life data tool. As the cosmic ray failure is random and occurs during the normal life of the component, the distribution was selected as 1P-exponential. 1-P exponential life distribution [55] is commonly used for failures with constant failure rates, which is also the case with cosmic ray failures. Six modules were marked as failed within their corresponding failure time frame and the rest of the modules were marked as suspended. A confidence level of 95 % was selected to be sufficient for presenting the results. This confidence level has also been used in cosmic ray testing in [4, 35, 36]. The results from the calculation showed a good match with the accelerated test results from manufacturer A.

The test is planned to be continued with the remaining DUTs to give more reliability to the results and to see how the failure rate will develop. The test setup could also be moved to an underground lab to see whether the failure rate would decrease as was seen in [6]. Adding more similar rated power semiconductor modules from other manufacturers to this test is also being considered. It would be interesting to see how a component, that has been estimated to have different cosmic ray robustness, would perform in a similar test. Lastly, the test setup could be modified by adding dynamic biasing as it is a more realistic operation scenario for power semiconductors.

5. METHODS FOR REDUCING COSMIC RAY FAILURES

As power semiconductor applications are getting more demanding, cosmic ray failures have become relevant in a broad range of industries. This has led to research work on ways to improve radiation robustness. One already mentioned method is to increase the thickness of the drift region in the power electronic chip, but this leads to increased losses in the forward conduction mode and/or increased turn-off losses [3]. Also, the base material has been seen to adjust the voltage threshold for cosmic ray failures and will be discussed in more detail below. Another option that does not particularly affect the device design is the shielding that can be placed around the power semiconductor.

5.1 Shielding

Shielding means attenuation of radiation and can be done by surrounding the power semiconductor device with a shielding material. This requires different widths of shielding depending on the material used (Figure 24). As a practical example, devices operated underground or surrounded by massive concrete walls do not face cosmic ray failures [12].

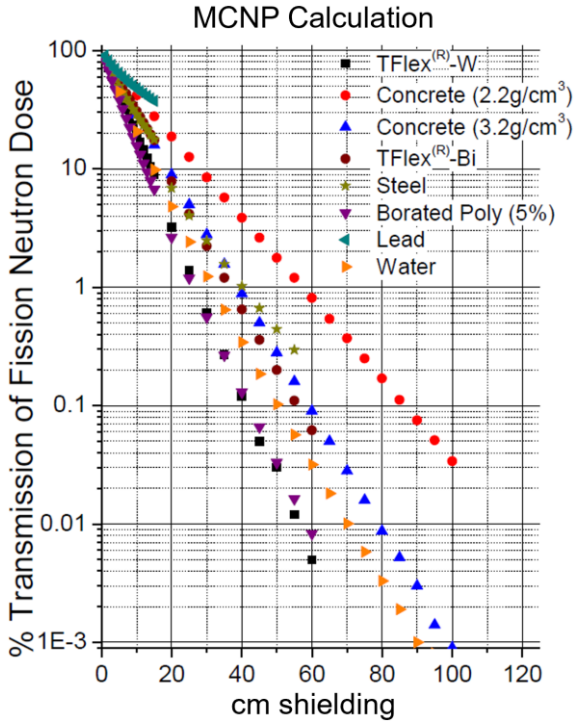

Figure 24. *Effectiveness of different shielding materials [54]*

Neutrons are most effectively shielded by materials with low density and high hydrogen content, such as water or high-density polyethylene. These materials reduce the energy/speed of neutrons (thermalize) and can change the shape of the neutron energy spectrum [39]. Thermalization happens as a cause of scattering interactions which are in hydrogen more effective than in other elements. Thermalization also produces secondary radiation so typically shielding materials include elements with high neutron absorption cross sections, such as boron. Boron absorbs thermalized neutrons and reduces secondary radiation production during neutron capture. [54]

The question regarding shielding is whether the material can effectively attenuate neutrons with energies of 50-200 MeV as they were told to be responsible for cosmic ray failures in power semiconductors [12]. For example, in a large building, it was found that two 15-cm concrete slabs reduced the high-energy portion (>10 MeV) of the neutron spectrum by a factor of 2.3 while the total neutron flux was reduced by a factor of 1.6 [39]. Also, steel or other materials with high atomic number is told to have a chance to significantly distort the neutron spectrum [39]. Another research was done in [2] and the failure rate was seen to decrease when tested devices were moved from a laboratory with a tin roof to a basement with 2.5 m concrete.

Selecting the best material for cosmic ray shielding depends on attenuation properties, chemical and physical compatibility, weight and budget limitations, and potential neutron activation of shielding materials [54]. Determining the shielding effect can be a difficult task and Monte Carlo N-Particle (MCNP) [44] calculations should be done to model the attenuation for different types of buildings and enclosures [39].

5.2 Layer design

Layer design is one example of a method that has the potential to reduce cosmic ray failures. Some experiments have shown that the SEB threshold increases with the drift-region thickness (Figure 25). One could say that an easy way to get around cosmic ray failures would be to make thick power electronic chips, but this would heavily increase the on-state losses. However, high-voltage power semiconductors tend to have thicker drift regions which have a positive effect on cosmic ray robustness. [22]

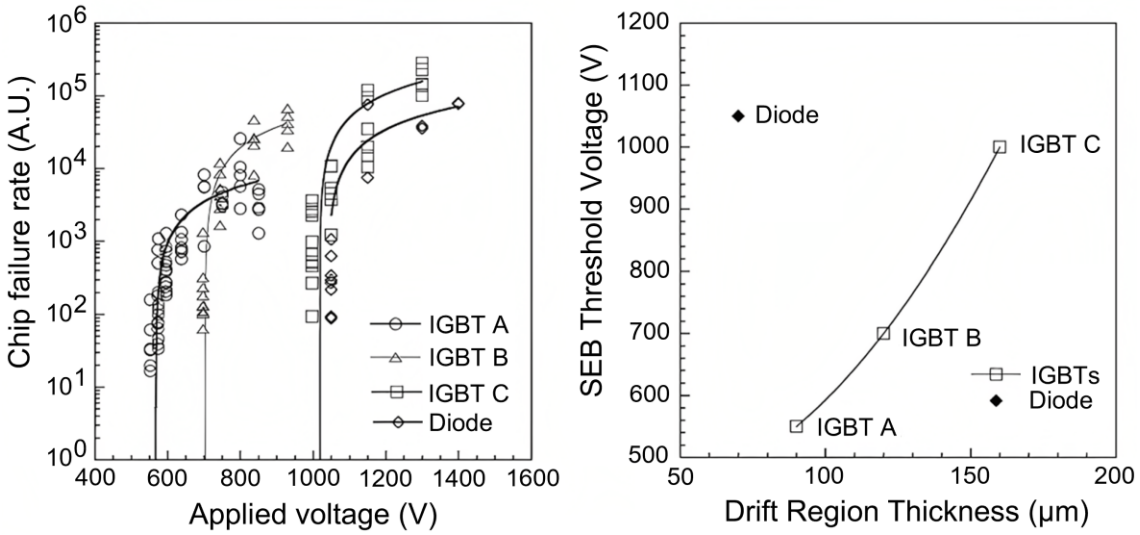

Figure 25. *Chip failure rate vs applied bias voltage and SEB threshold voltage vs drift-region thickness [22]*

An additional layer called Deep-N buffer layer (DN) was introduced in 2020 to improve radiation robustness in an IGBT without increasing the thickness of the base material. Simulations in TCAD showed that DN suppresses bipolar PNP action and the temperature rising around P-collector. Experimental results in the facility of the Research Center for Nuclear physics (RCNP) at Osaka University verified the improvement of robustness. In these tests, an IGBT with the proposed DN structure was manufactured and compared to a conventional IGBT (Figure 26). The structure in Figure 26 includes a shallow-N layer which can also be denoted as a field-stop layer. Field-stop layer is typically included in all modern IGBTs. [32]

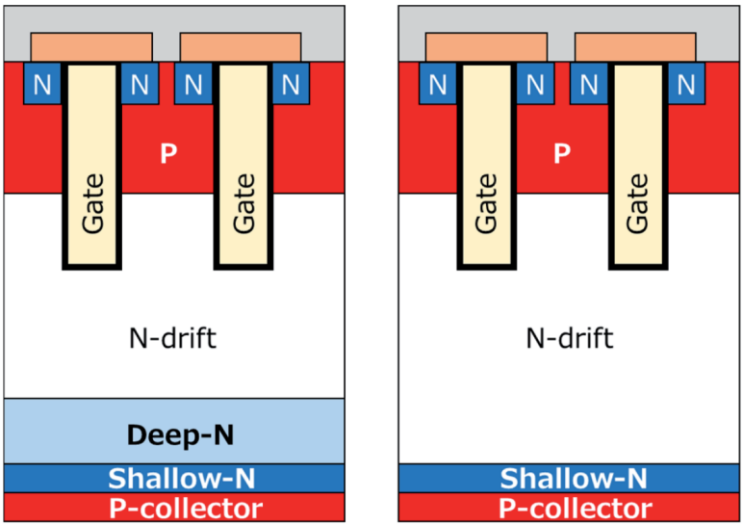

Figure 26. *IGBT structures: w-DN on the left, w/o-DN on the right [32]*

The tested IGBTs irradiated with white neutron beams at RCNP. The neutron beams at RCNP have similar energy spectrums compared to NYC sea level and are thus valid for

failure rate testing. During the test, DUTs are exposed to high voltages and the gate-emitter is short-circuited to assure the blocking state throughout the test. Also, the leakage current is monitored to detect failures by measuring the voltage over a shunt resistor (Figure 27). [32]

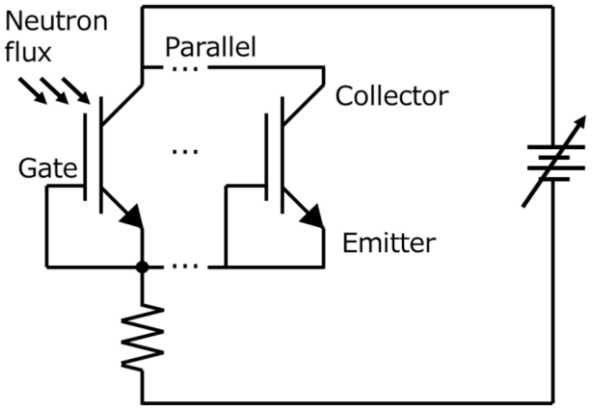

Figure 27. *Test circuit for cosmic ray failures using white neutron beams [32]*

This is a typical test circuit for accelerated SEB testing and is quite like the test setup at Vaasa. Experimental results from the tests in [32] are presented in Figure 28 at the collector-emitter voltage (V_{CE}) region near 2/3 of the rated voltage, which is often seen as the threshold for an exponential increase in failures for a power semiconductor.

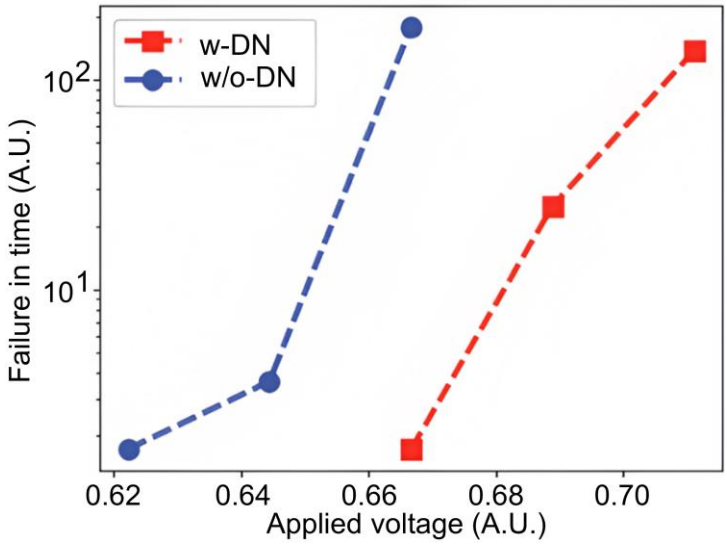

Figure 28. *Experimental results for IGBT w-DN and w/o-DN [32]*

Taken that 100 FIT would be the requirement for a power semiconductor device, at that FIT the conventional IGBT has an applied V_{CE} of 0.66 and with the DN a V_{CE} of 0.71. For example, for 1200 V modules this transforms to V_{CE} increase from 790 V to 850 V. As a conclusion, the improvement introduced by the DN layer is significant. However, now there seems to be no more public knowledge on this design and how it could affect the electrical performance of the IGBT.

5.3 Voltage rating selection

Solar central converter applications are having a trend toward a DC-link voltage of 1500 V. One of the most important aspects of these high-voltage applications is the robustness for cosmic ray failures which is also the reason why 1.7 kV devices might be impossible to use reliably at least for Si-based components. However, SiC-based components of this voltage rating have shown lower FIT rates in [33]. Another option would be to use power semiconductors with higher voltage ratings e.g., 2.2-2.5 kV.

In [56] experimental characteristics were designed for IGBT and diode chip set for safe operation under hard switching conditions at 2.8 kV DC voltage level. This chipset was aimed to get a low cosmic ray failure rate when having all the common requirements of low static and dynamic losses. Also, a wide safe operating area under turnoff, reverse recovery, and short-circuit conditions were fulfilled. The blocking capability of this chipset was reported to exceed 4.5 kV. [56]

In July 2020 at PCIM digital days new Si IGBT and Si diode technologies of voltage class 2.3 kV were presented. These chips were designed for solar central converter applications on MW-range with a DC-link voltage of 1500 V. The IGBT was based on Infineon's most recent TRENCHSTOP™ IGBT7 technology and adapted to the needs of a solar application. The diode was also from Infineon, based on their most recent emitter-controlled 7th generation technology and optimized for the usage as FWD for the 2.3 kV IGBT. These chips were designed to be operated in a standard 2-level topology or a 3-level neutral point clamped (NPC) topology when used in combination with a 1200 V module in a common collector configuration. [57]

5.4 Base material selection

For a long time, Si has been used in high-voltage power semiconductors as the base material. However, expensive SiC has reduced in price recently and come to the consideration as a valid option for Si. SiC offers advantages because of its drift properties, which allow devices to have high blocking voltage with lower conduction and switching losses. Regarding the tradeoff with electrical properties, cosmic ray robustness needs to be acknowledged as well for different base materials. [11, 58]

Silicon carbide is claimed to have a critical electric field three times higher than silicon [16]. This already indicates the better radiation robustness of SiC. Furthermore, the higher electric field withstand ability allows SiC chips to be thinner compared to similar voltage-rated Si chips. This could be accounted for the total area of the power semiconductor component. Also, SiC induces less losses and requires less area to maintain the

temperature at a tolerable level [32]. The smaller the area of the chip, the lower the probability to get destroyed by cosmic rays [11, 16, 32, 58].

In [11] a universal scaling approach was found when Wolfspeed SiC MOSFETs were tested for cosmic ray failures (Figure 29). These tests were done at LANSCE with up to 12 samples per test and the failure times were averaged for each drain bias voltage. Some variation was observed in the results, but this was explained by the small variation in devices' drift fields and the small sample size. In addition, devices from different manufacturers were tested and the same behavior was seen (Figure 29). [11]

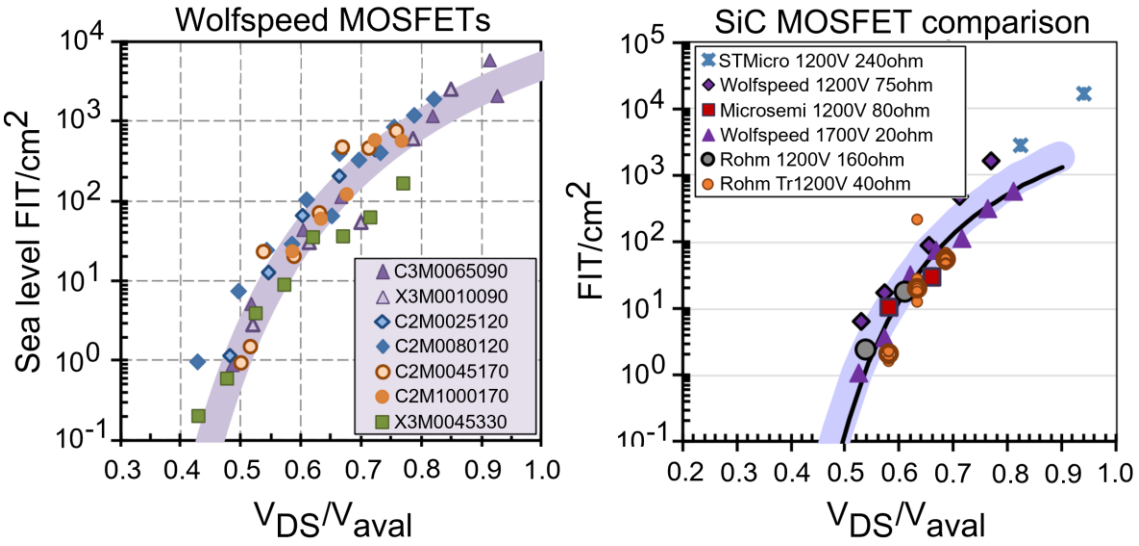

Figure 29. *The cosmic ray failure rate for Wolfspeed SiC MOSFETs (left) and other manufacturers (right) scaled by avalanche voltage [11]*

Tests were continued for SiC diodes and again the universal scaling factor was observed and indicated that the SiC drift properties dominate the failure rate for both SiC MOSFETs and diodes. From these observations, the significance of parasitic NPN transistor turn-on in failure mechanism is claimed to be minimal [11]. This conflicts with findings in [21, 22, 23], where the triggering of the parasitic NPN transistor was told to be one of the main reasons for SEB failures. This indicates that Si and SiC power MOSFETs could have different failure mechanisms triggered by cosmic rays and it might be due to differences in material, channel-oxide interface, or device layout [16].

In [36] this universal trend was investigated for even more SiC power MOSFETs and IGBTs. It was found that with V_{DS}/V_{aval} (avalanche voltage) ratios between 0.6 and 0.8 there can be a difference depending on the technology and the design of the device. Also, tests in [11] confirmed that device design affects the radiation robustness but that the most dominant factors in SiC power MOSFETs are the active blocking area and the SiC drift properties. An interesting note made in [36] was that Si power MOSFETs and IGBTs did not follow a common trend. However, these tests were done at ChipIr which

has a different neutron spectrum compared to tests done in [11] at LANSCE. Some of the test results at ChipIr are presented in Figure 30.

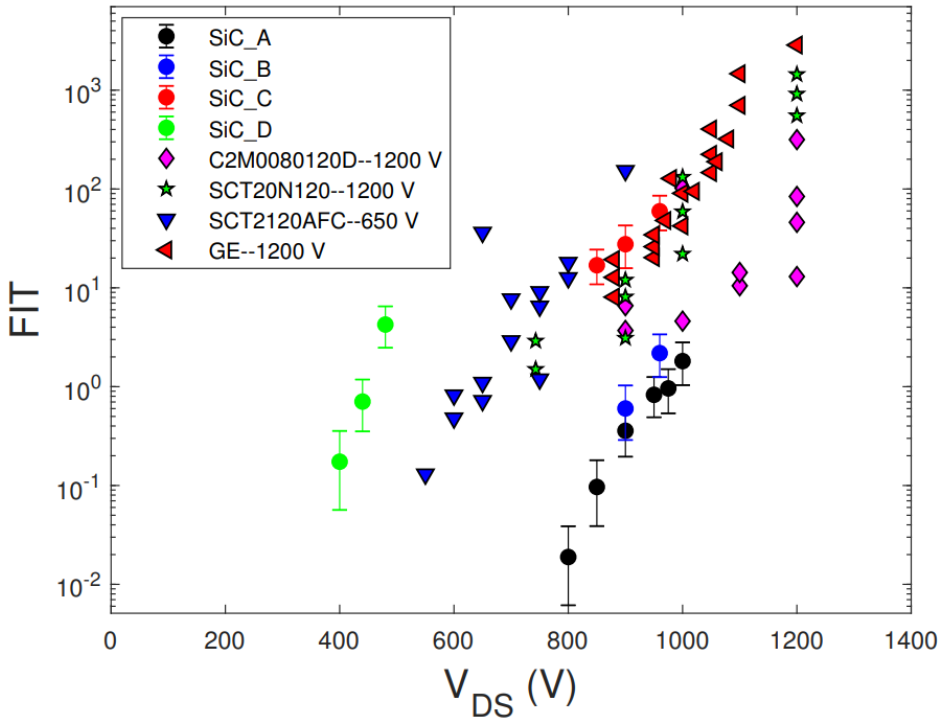

Figure 30. *SiC MOSFET failure rate data, SiC_A-C (1200 V STMicro) and SIC_D (650 V STMicro) from [36]. Data of the commercial SiC MOSFETs C2M0080120D (1200 V Wolfspeed), SCT20N120 (1200 V STMicro), and SCT2120AFC (650 V ROHM) from [16] and GE-1200 V from [59].*

From Figure 30 it is visible that power MOSFETs with a lower voltage rating see failures at lower voltages compared to the higher-rated ones. For 650 V devices, ROHM seems to have better radiation robustness compared to STMicroelectronics. 650 V ROHM seems to face cosmic ray FITs at a notable level only when going beyond the rated voltage. In the category of 1200 V devices, STMicroelectronics has a variation of up to a decade between its devices' failure rates and Wolfspeed seems to fall behind GE and STMicroelectronics in robustness at rated voltage. This is by no means a good indicator between manufacturers to see who makes devices with better cosmic ray withstanding abilities because as seen with STMicroelectronics, a big difference exists between different designs. Another note to make is that the failure data from [16, 59] do not have a confidence level considered, whereas in data from [36] a 95 % confidence level was acknowledged.

For a comparison, Si power MOSFETs were also tested in [36]. The results concluded that Si has a higher chance for cosmic ray failures compared to SiC. This is also supported by tests and comparisons done in [11, 16, 18, 33] for power MOSFETs and in [11, 33] for diodes.

6. CONCLUSIONS

This thesis began by introducing cosmic rays and the possible failure mechanisms that they can trigger in power semiconductors. Regarding high-power semiconductors, neutrons with energies between 50 and 250 MeV were told to be responsible for the failures. Failures in diodes occurred by impact ionization causing a streamer inside the chip but the same principle applies to other components as well. It was seen that different component types introduce additional failure mechanisms that can become dominant e.g., the triggering of the parasitic PNP or NPN transistor in an IGBT.

The thesis proceeded to discuss the affecting factors for cosmic ray failures. These were the blocking voltage, junction temperature, and neutron flux. It was seen that the failure amounts increase exponentially above a certain voltage threshold, usually 2/3 of the rated collector-emitter voltage. It was also seen that the increase in the junction temperature has a decreasing effect on the failure rate. The neutron flux was concluded to be a major factor in the failure rate, and it was seen to be highly dependent on altitude, latitude, and solar activity.

Then some empirical models, Zeller, Pfirsch, and Kaminski were discussed for quantifying cosmic ray robustness early in the development phase of the power semiconductors. The shape of the failure rate curve calculated with the Kaminski model differed from the other two models and the Pfirsch model seemed to give more accurate failure rates at low voltages compared to the Zeller model. The varying results showed the need for testing with real hardware when accurate failure rates are required. However, these models are beneficial for comparing e.g., the effect of changing layer thicknesses when the electric field distribution is known. Also, simulation was discussed briefly, and Monte Carlo techniques were concluded to be effectively combined with TCAD simulations in modeling the cosmic ray robustness of power semiconductors.

The next subject was cosmic ray failure testing which introduced storage tests with natural terrestrial flux and accelerated tests with artificial neutron and proton beams. The effects of constant high voltage and switching during the tests were discussed. Previous research had shown that a constant high voltage for multiple months could result in increased failure rates that tend to locate near the edges of the chips. Also, dynamic biasing was concluded to be a more realistic test scenario for power semiconductors and that including the overvoltage peaks during the cut-off of current would increase the failure rates.

A test setup was developed in this thesis for cosmic ray testing and multiple test samples from one manufacturer were included in the test. The preliminary plan for the test setup was to verify the failure rate estimated by the manufacturer through tests with artificial radiation sources. The first results showed a good match with the estimate from accelerated tests but the reason for failures could not yet be justified as cosmic rays. However, this was a good introduction to this type of testing and multiple continuation ideas were presented to mitigate uncertainty regarding the origin of the failure.

The last topic for the thesis was to present some methods to reduce the probability of cosmic ray failures. Shielding was acknowledged as the only method that can be done externally from the component point of view. Hydrogen was seen to be an effective neutron attenuator according to MCNP calculations and discussions with the personnel at Oulu Cosmic Ray Station. However, for the shielding to be effective, it seemed that thick layers of shielding material are required independent of the material. Regarding the improvement of internal properties of the components for radiation robustness, especially the width of the drift layer was seen to have an impact. In addition to this, the positive impact of a rather new invention, the Deep-N layer, was discussed. Also, using power semiconductors of higher voltage rating was concluded to be effective for getting more margin for cosmic ray stability. Lastly, some research results were presented for comparison of Si and SiC. The latter concluded to have better cosmic ray robustness.

REFERENCES

[1] J.F. Ziegler, “Terrestrial Cosmic Rays”, IBM journal of research and development, Vol. 40, No. 1, pp. 19-39, 1996.

[2] H. Kabza et al., “Cosmic Radiation as a Cause for Power Device Failure and Possible Countermeasures”, Proceedings of the 6th International Symposium on Power Semiconductor Devices and ICs, IEEE, pp. 9-12, 1994.

[3] J. Lutz et al., “Semiconductor Power Devices: Physics, Characteristics, Reliability”, Springer International Publishing AG, 2018.

[4] U. Scheuermann, U. Schilling, “Impact of Device Technology on Cosmic Ray Failures in Power Modules”, IET power electronics, Vol. 9, No. 10, pp. 2027-2035, 2016.

[5] ABB, “Failure rates of IGBT modules due to cosmic rays”, Application Note 5SYA 2042–09, 2019.

[6] F. Pfirsch, G. Soelkner, “Simulation of Cosmic Ray Failures Rates Using Semiempirical Models”, 22nd International Symposium on Power Semiconductor Devices and ICs, IEEE, pp. 125–128, 2010.

[7] H.R. Zeller, “Cosmic Ray Induced Failures in High Power Semiconductor Devices”, Solid State Electronics, Vol. 38, No. 12, pp. 2041–2046, 1995.

[8] G. Soelkner et al., “Reliability of Power Electronic Devices Against Cosmic Radiation-Induced Failure”, Microelectronics and reliability, Vol. 44, No. 9, pp. 1399–1406, 2004.

[9] C. Findeisen et al., “Extrapolation of Cosmic Ray Induced Failures from Test to Field Conditions for IGBT Modules”, Microelectronics and reliability, Vol. 38, No. 6, pp. 1335–1339, 1998.

[10] Los Alamos National Laboratory n.d., LANSCE Radiation Effects Facilities, accessed 2 December 2022. Available: https://lansce.lanl.gov/facilities/Radiation%20Effects/index.php

[11] S. Allen et al., “Reliability of SiC Power Devices Against Cosmic Ray Neutron Single-Event Burnout”, Materials science forum, Vol. 924, pp. 559–562, 2018.

[12] G. Soelkner, “Ensuring the Reliability of Power Electronic Devices with Regard to Terrestrial Cosmic Radiation”, Microelectronics and reliability, Vol. 58, pp. 39–50, 2016.

[13] T.J. Dunai, “Cosmogenic Nuclides: Principles, Concepts and Applications in the Earth Surface Sciences”, Cambridge University Press, 2010.

[14] M.S. Gordon et al., “Measurement of the Flux and Energy Spectrum of Cosmic-Ray Induced Neutrons on the Ground”, IEEE transactions on nuclear science, Vol. 51, No. 6, pp. 3427–3434, 2004.

[15] C. Weiss et al., “Numerical Analysis of Cosmic Radiation-Induced Failures in Power Diodes” Proceedings of the European Solid-State Device Research Conference, IEEE, pp. 355–358, 2011.

[16] A. Akturk et al., “Single Event Effects in Si and SiC Power MOSFETs Due to Terrestrial Neutrons”, IEEE transactions on nuclear science, Vol. 64, No. 1, pp. 529–535, 2017.

[17] Semikron, “Cosmic Ray Failures in Power Electronics”, Application Note AN 17-003, 2017.

[18] G. Consentino et al., “Are SiC HV power MOSFETs more robust of standard silicon devices when subjected to terrestrial neutrons?”, Proceedings of PCIM Europe (Nuremberg, Germany), pp. 512–517, 2015.

[19] C. Weiß, “Höhenstrahlungsresistenz von Silizium-Hochleistungs-bauelementen”, Ph.D. Thesis, The Technical University of Munich, 2015.

[20] T. Shoji, et al., “Triggering mechanism for neutron induced single-event burnout in power devices”, Japanese Journal of Applied Physics, Vol. 52, No. 4, pp. 04CP06-1– 04CP06-7, 2013.

[21] T. Oda et al., “Electric-Field-Dependence Mechanism for Cosmic Ray Failure in Power Semiconductor Devices”, IEEE transactions on electron devices, Vol. 68, No. 7, pp. 3505–3512, 2021.

[22] T. Shoji et al., “Cosmic Ray Neutron-Induced Single-Event Burnout in Power Devices”, IET power electronics, Vol. 8, No. 12, pp. 2315–2321, 2015.

[23] T. Shoji et al., “Observation and Analysis of Neutron-Induced Single-Event Burnout in Silicon Power Diodes”, IEEE transactions on power electronics, Vol. 30, No. 5, pp. 2474–2480, 2015.

[24] S. Wender, L. Dominik, “Los Alamos High-Energy Neutron Testing Handbook”, 2020.

[25] T. Nitta et al., “Cosmic Ray Failure Mechanism and Critical Factors for 3.3kV Hybrid SIC Modules”, PCIM Europe; International Exhibition and Conference for Power Electronics, Intelligent Motion, Renewable Energy and Energy Management, pp. 566–572, 2016.

[26] M. Domeij et al., “On the Destruction Limit of Si Power Diodes During Reverse Recovery with Dynamic Avalanche”, IEEE transactions on electron devices, Vol. 50, No. 2, pp. 486–493, 2003.

[27] J. Lutz, M. Domeij, “Dynamic Avalanche and Reliability of High Voltage Diodes”, Microelectronics and reliability, Vol. 43, No. 4, pp. 529–536, 2003.

[28] A. Fayyaz et al., “UIS Failure Mechanism of SiC Power MOSFETs”, 4th Workshop on Wide Bandgap Power Devices and Applications, IEEE, pp. 118–122, 2016.

[29] J. Salonen, ”IGBT-transistori”, B.S. Thesis, Tampere University of Applied Sciences, 2013.

[30] S. Nishida et al., “Cosmic Ray Ruggedness of IGBTs for Hybrid Vehicles”, 22nd International Symposium on Power Semiconductor Devices & ICs, IEEE, pp. 129–132, 2010.

[31] J.F. Ziegler, “Terrestrial Cosmic Ray Intensities”, IBM journal of research and development, Vol. 42, No. 1, pp. 117–139, 1998.

[32] D. Yoshikawa et al., “Improvement of Cosmic Ray Robustness in IGBT with Deep-N Layer”, Proceedings of the International Symposium on Power Semiconductor Devices and ICs, pp. 486–489, 2020.

[33] C. Felgemacher et al., “Benefits of Increased Cosmic Radiation Robustness of SiC Semiconductors in Large Power-Converters”, PCIM Europe; International Exhibition and Conference for Power Electronics, Intelligent Motion, Renewable Energy and Energy Management, pp. 573–580, 2016.

[34] C. Felgemacher et al., “Cosmic Radiation Ruggedness of Si and SiC Power Semiconductors”, Proceedings of the International Symposium on Power Semiconductor Devices and ICs, pp. 51–54, 2016.

[35] U. Scheuermann, U. Schilling, “Cosmic Ray Failures of Power Modules -The Diode Makes the Difference” PCIM Europe; International Exhibition and Conference for Power Electronics, Intelligent Motion, Renewable Energy and Energy Management; Proceedings of, 2015.

[36] F. Principato et al., “Accelerated Tests on Si and SiC Power Transistors with Thermal, Fast and Ultra-Fast Neutrons”, Sensors, Vol. 20, No. 11, pp. 3021–, 2020.

[37] D. Wilkinson 2012, Space environment overview, accessed 2 December 2022. Available: https://commons.wikimedia.org/wiki/File:SpaceEnvironmentOverview_From_19830101.jpg

[38] Cosmic Ray Station of the University of Oulu 2022, Oulu Neutron Monitor, accessed 2 December 2022. Available: https://cosmicrays.oulu.fi/

[39] JEDEC Std., “JESD89A: Measurement and Reporting of Alpha Particle and Terrestrial Cosmic Ray-Induced Soft Errors in Semiconductor Devices”, 2006.

[40] J. Wilkinson 2006, Soft-error Testing Resources, accessed 2 December 2022. Available: http://seutest.com/cgi-bin/FluxCalculator.cgi

[41] A. Akturk et al., “Predicting Cosmic Ray-Induced Failures in Silicon Carbide Power Devices”, IEEE transactions on nuclear science, Vol. 66, No. 7, pp. 1828–1832, 2019.

[42] D.R. Ball et al. “Estimating Terrestrial Neutron-Induced SEB Cross Sections and FIT Rates for High-Voltage SiC Power MOSFETs”, IEEE transactions on nuclear science, Vol. 66, No. 1, pp. 337– 343, 2019.

[43] S. Katoh et al., “Temperature Dependence of Single-Event Burnout for Super Junction MOSFET”, 27th International Symposium on Power Semiconductor Devices & IC’s, IEEE, pp. 93–96, 2015.

[44] Los Alamos National Laboratory 2022, The MCNP® Code, accessed 2 December 2022. Available: https://mcnpx.lanl.gov/

[45] Deutsches Zentrum für Luft- und Raumfahrt 2021, Detector measures cosmic radiation on the Zugspitze, accessed 2 December 2022. Available: https://dlr.de/content/en/articles/news/2021/02/20210616_detector-measures-cosmic-radiation-on-the-zugspitze.html

[46] H.H.K. Tang, “Nuclear physics of cosmic ray interaction with semiconductor-materials: particle-induced soft errors from a physicist’s perspective”, IBM journal of research and development, Vol. 40, No. 1, pp. 91–108, 1996.

[47] C.W. Slayman, “Theoretical Correlation of Broad Spectrum Neutron Sources for Accelerated Soft Error Testing”, IEEE transactions on nuclear science, Vol. 57, No. 6, pp. 3163–3168, 2010.

[48] A. Haertl et al., “Influence of Dynamic Switching on the Robustness of Power Devices Against Cosmic Radiation”, 24th International Symposium on Power Semiconductor Devices and ICs, IEEE, pp. 353–356, 2012.

[49] Z. Torok et al., “SEE-Inducing Effects of Cosmic Rays at the High-Altitude Research Station Jungfraujoch Compared to Accelerated Test Data”, 9th European Conference on Radiation and Its Effects on Components and Systems, IEEE, pp. 1–6, 2007.

[50] F. Lei et al., “An Atmospheric Radiation Model Based on Response Matrices Generated by Detailed Monte Carlo Simulations of Cosmic Ray Interactions”, IEEE transactions on nuclear science, Vol. 51, No. 6, pp. 3442–3451, 2004.

[51] C. Cazzaniga, C.D. Frost, “Progress of the Scientific Commissioning of a Fast Neutron Beamline for Chip Irradiation”, 22nd Meeting of the International Collaboration on Advanced Neutron Sources, Vol. 1021, No. 1, pp. 12037–, 2018.

[52] A.V. Prokofiev et al. “Characterization of the ANITA Neutron Source for Accelerated SEE Testing at the Svedberg Laboratory”, Radiation Effects Data Workshop, IEEE, pp. 166–173, 2009.

[53] E.W. Blackmore et al., “Improved Capabilities for Proton and Neutron Irradiations at TRIUMF”, Radiation Effects Data Workshop Record, IEEE, pp. 149–155, 2003.

[54] Eichrom Technologies Inc. 2016, Neutron Radiation: The Concern, Reason, and Solution, accessed 2 December 2022. Available: https://www.eichrom.com/npo/latest-news/neutron-radiation-the-concern-reason-and-solution/

[55] ReliaWiki 2013, Life Distributions, accessed 2 December 2022. Available: https://reliawiki.org/index.php/Life_Distributions

[56] F. Bauer et al., “A High Voltage IGBT and Diode Chip Set Designed for the 2.8 kV DC Link Level with Short Circuit Capability Extending to the Maximum Blocking Voltage”, International Symposium on Power Semiconductor Devices and ICs, IEEE, pp. 29–32, 2000.

[57] F. Umbach et al., “2.3 kV - A New Voltage Class for Si IGBT and Si FWD”, PCIM Europe Conference Proceedings, Vol. 1, pp. 248–254, 2020.

[58] J.H. Park et al., “Accelerated Testing of SiC Power Devices Under High-Field Operating Conditions”, Materials science forum, Vol. 1004, pp. 992–997, 2020.

[59] A. Bolotnikov et al., “Overview of 1.2kV - 2.2kV SiC MOSFETs Targeted for Industrial Power Conversion Applications”, Applied Power Electronics Conference and Exposition, IEEE, pp. 2445–2452, 2015.